

12

AFGL-TR-82-0039

AD A118775

SOLAR RADIATIVE FLUX CALCULATIONS FROM  
STANDARD SURFACE METEOROLOGICAL OBSERVATIONS

Ralph Shapiro

Systems and Applied Sciences Corporation (SASC)  
6811 Kenilworth Avenue  
Riverdale, MD 20737

MARCH 1, 1982

Scientific Report No. 1

Approved for public release; distribution unlimited

AIR FORCE GEOPHYSICS LABORATORY  
AIR FORCE SYSTEMS COMMAND  
UNITED STATES AIR FORCE  
HANSCOM AFB, MASSACHUSETTS 01731

DTIC FILE COPY

DTIC  
SELECTED  
AUG 31 1982  
E

Qualified requestors may obtain additional copies from the Defense Technical Information Center. All others should apply to the National Technical Information Service.

UNCLASSIFIED

SECURITY CLASSIFICATION OF THIS PAGE (When Data Entered)

REPORT DOCUMENTATION PAGE		READ INSTRUCTIONS BEFORE COMPLETING FORM						
1. REPORT NUMBER AFGL-TR-82-0039	2. GOVT ACCESSION NO. AD-A118775	3. RECIPIENT'S CATALOG NUMBER						
4. TITLE (and Subtitle)  SOLAR RADIATIVE FLUX CALCULATIONS FROM STANDARD SURFACE METEOROLOGICAL OBSERVATIONS		5. TYPE OF REPORT & PERIOD COVERED Scientific Report No. 1						
		6. PERFORMING ORG. REPORT NUMBER						
7. AUTHOR(s)  Ralph Shapiro		8. CONTRACT OR GRANT NUMBER(s)  F19628-81-C-0042						
9. PERFORMING ORGANIZATION NAME AND ADDRESS Systems and Applied Sciences Corporation 6811 Kenilworth Avenue P.O. Box 308 Riverdale, MD 20737		10. PROGRAM ELEMENT, PROJECT, TASK AREA & WORK UNIT NUMBERS 63707F 268802AB						
11. CONTROLLING OFFICE NAME AND ADDRESS AIR FORCE GEOPHYSICS LABORATORY HANSCOM AFB, MA 01731 Manager/Lt Col Kit G. Cottrell/OPI		12. REPORT DATE March 1, 1982						
		13. NUMBER OF PAGES 53						
14. MONITORING AGENCY NAME & ADDRESS (if different from Controlling Office)		15. SECURITY CLASS. (of this report)  UNCLASSIFIED						
		15a. DECLASSIFICATION/DOWNGRADING SCHEDULE						
16. DISTRIBUTION STATEMENT (of this Report)  Approved for public release; distribution unlimited.								
17. DISTRIBUTION STATEMENT (of the abstract entered in Block 20, if different from Report)								
18. SUPPLEMENTARY NOTES								
19. KEY WORDS (Continue on reverse side if necessary and identify by block number)  <table border="0"> <tr> <td>Solar radiation</td> <td>Cloud reflectance</td> </tr> <tr> <td>Flux calculations</td> <td>Cloud absorptance</td> </tr> <tr> <td>Solar insolation model</td> <td>Cloud transmittance</td> </tr> </table>			Solar radiation	Cloud reflectance	Flux calculations	Cloud absorptance	Solar insolation model	Cloud transmittance
Solar radiation	Cloud reflectance							
Flux calculations	Cloud absorptance							
Solar insolation model	Cloud transmittance							
20. ABSTRACT (Continue on reverse side if necessary and identify by block number)  <p>The flux of solar radiation through a model atmosphere composed of <math>n</math> layers and a ground surface is represented by a system of <math>2n+2</math> linear equations. The system is solved in closed form explicitly for the radiation reaching the ground and the radiation reflected back to space, as a function of the vertically incident radiation and specified reflection and transmission coefficients for each of the <math>n</math> layers and the ground. These coefficients vary in time and space as functions of a wide variety of parameters. However, they are primarily dependent upon cloud amount and cloud thickness or type. In spite of,</p>								

DD FORM 1 JAN 73 1473 EDITION OF 1 NOV 65 IS OBSOLETE

UNCLASSIFIED

SECURITY CLASSIFICATION OF THIS PAGE (When Data Entered)

UNCLASSIFIED

SECURITY CLASSIFICATION OF THIS PAGE(When Data Entered)

some past measurement programs, the cloud coefficients are not very well known. Making use of direct observations of the total solar radiation reaching the ground and simultaneous cloud observations, the model offers the opportunity for determining the mean transmission and reflection characteristics of any individual cloud type.

The model is flexible with regard to the number of layers chosen to represent the atmosphere and with regard to the sophistication of the physics to be incorporated. With the use of the SOLMET data tapes, a first approximation calculation is described for the reflection, transmission, and absorption coefficients for a three-layer atmosphere containing high, middle, and low cloud types. Once these coefficients have been determined, the flux of solar radiation is calculated from routine surface meteorological observations. A test of the model on independent data shows no loss in accuracy as compared with that obtained with the developmental data sample.

UNCLASSIFIED

SECURITY CLASSIFICATION OF THIS PAGE(When Data Entered)

[illegible]

•

I would like to express my appreciation and admiration to Mr. Randy Schechter for his able handling of the voluminous computations in his role as intermediary with the computer.

DIIC  
COPY  
NOTATED  
2

## TABLE OF CONTENTS

1. INTRODUCTION . . . . .	5
2. MODEL STRUCTURE . . . . .	8
3. REFLECTIVITY, TRANSMISSIVITY AND ABSORPTIVITY COEFFICIENTS . . . . .	16
4. WEIGHTING FUNCTION FOR FRACTIONAL CLOUD COVER . . . . .	29
5. APPLICATION OF THE MODEL . . . . .	35
6. ANALYSIS OF ERROR AND CONCLUSIONS . . . . .	40
REFERENCES . . . . .	50

## 1. INTRODUCTION

Although knowledge of the amount of solar radiation absorbed and reflected back to space by the ground and atmosphere is pertinent to a large variety of geophysical processes, the application for which the present procedure has been formulated involves the heat balance of terrestrial objects and backgrounds. The application requires a simple means to approximate the flux of both upward- and downward-directed solar radiation through the atmosphere using only routine surface weather observations. These requirements have served to limit and focus the structure of the procedure. Although the downward flux of solar radiation at the ground is the only parameter which is specifically required, this flux, as well as each of the fluxes at all levels, is dependent upon all of the fluxes. This means that it is necessary, at least implicitly, to know or to solve for all of the fluxes in order to obtain any of the fluxes. Thus, in obtaining the downward flux of solar radiation at the ground, one also has available the amount of radiation absorbed in the atmosphere and reflected back to space.

The author had developed (Shapiro, 1972)<sup>1</sup> a simple model for the flux of solar radiation through the atmosphere which was readily adaptable for the present purpose. The model, however, requires knowledge of the coefficients of reflectivity, transmissivity and absorptivity of each of the  $n$ , plane-parallel layers into which the atmosphere is divided. Furthermore, since these coefficients are most sensitive to variations in cloud type and amount, knowledge of the absorption, reflection and transmission of solar radiation for individual cloud types is particularly necessary. Ultimately, such knowledge must be based upon direct observation. Perhaps the most satisfactory approach is the direct observation of reflection, transmission and absorption of individual clouds from instrumented aircraft. Unfortunately, such measurements are difficult and expensive and there exists today only a limited number of such measurements for a limited number of cloud types. Although there have been some recent measurements (Paltridge and Platt, 1981<sup>2</sup>; Reynolds et al., 1975<sup>3</sup>; Paltridge, 1973<sup>4</sup> and 1974<sup>5</sup>; Cox et al., 1973<sup>6</sup>; Drummond and Hickey, 1971<sup>7</sup>), and some not so

---

Because of the number of references to be included as footnotes on this page, the reader is referred to the list of references, page 50.

recent (Feigel'son, 1966<sup>8</sup>; Predoehl and Spano, 1965<sup>9</sup>; Hanson and Viebrock, 1964<sup>10</sup>), much of the available information was obtained more than 20 years ago (Roach, 1961<sup>11</sup>; Robinson, 1958<sup>12</sup>; Fritz and MacDonald, 1951<sup>13</sup>; Fritz, 1950<sup>14</sup>; Neiburger, 1949<sup>15</sup>).

In addition to these measurements, there have been some direct measurements of cloud microphysics, such as those of Reynolds et al. (1978)<sup>16</sup>, Platt (1976)<sup>17</sup>, Paltridge (1974)<sup>5</sup>, among others. These measurements of drop-size distribution and liquid water content have served as the basis for a large number of theoretical computations. Much of the present knowledge of the flux of solar radiation in the atmosphere and its variation under a variety of conditions is due to such computations, which are based both upon scattering theory and Monte Carlo calculations. The results of course are dependent upon the modeling assumptions which are made, but these in recent years have become increasingly sophisticated and presumably increasingly realistic. Prominent among these studies is the recent monograph by Welch et al. (1980)<sup>18</sup> which contains a large number and variety of computations. Other recent reviews are those of Van De Hulst (1980)<sup>19</sup>, Fouquart et al. (1980)<sup>20</sup> and Lenoble (1977)<sup>21</sup>. An indication of the volume and scope of such studies may be given by a sampling of some recent contributions: Newinger and Bähnke (1981)<sup>22</sup>; Platt (1981)<sup>23</sup>; Welch and Zdunkowski (1981a, b)<sup>24,25</sup>; Fouquart and Bonnel (1980)<sup>26</sup>; Leighton (1980)<sup>27</sup>; Manton (1980)<sup>28</sup>; Meador and Weaver (1980)<sup>29</sup>; Zdunkowski et al. (1980)<sup>30</sup>; Davis et al. (1979a, b)<sup>31,32</sup>; Liou and Wittman (1979)<sup>33</sup>; Schaller (1979)<sup>34</sup>; Schmetz and Raschke (1979)<sup>35</sup>; Stephens (1978,1979)<sup>36,37</sup>; Davies (1978)<sup>38</sup>; Kerschgens et al. (1978)<sup>39</sup>; Twomey (1976,1977)<sup>40,41</sup>; Wendling (1977)<sup>42</sup>; Wiscombe (1976a,b, 1977)<sup>43,44,45</sup>; Liou (1974,1976)<sup>46,47</sup>; McKee and Cox (1974,1976)<sup>48,49</sup>; Welch et al (1976)<sup>50</sup>; Wiscombe and Grams (1976)<sup>51</sup>; Zdunkowski and Korb (1974)<sup>52</sup>.

Although there are sizeable differences among the measurements and among the calculations for similar cloud conditions, the results, insofar as comparisons are feasible, are generally individually and mutually consistent. The central feature of both the studies and the direct measurements is the not unexpected result that the fractions of sunlight reflected, transmitted and absorbed are proportional to the density and thickness of the clouds, or in other words, are functions of cloud type.

Haurwitz (1948)<sup>53</sup>, by means of hourly cloud observations and coordinated solar insolation measurements, was able to obtain estimates of mean



transmissivity as a function of cloud type and solar zenith angle. Although there have been a number of similar studies in more recent years, such as Kasten and Czeplak (1980)<sup>54</sup>, Atwater and Ball (1978)<sup>55</sup>, Tabata (1964)<sup>56</sup>, Lumb (1964)<sup>57</sup>, Vowinckel and Orvig (1962)<sup>58</sup>, Haurwitz's extensive study remains definitive for its type. Nevertheless, Haurwitz's results were obtained from only eight years of data at Blue Hill, Massachusetts and are deficient in several cloud types, particularly for the larger zenith angles.

Theoretical model calculations have the advantage of completeness in that results can be obtained for any assumed set of cloud conditions. However these models are not suitable for routine computations since they require cloud microphysical information which is not routinely available. Furthermore, there have been too few coordinated measurements of cloud type and cloud microphysics to substitute cloud type for microphysics in these models. The present approach, which has been deliberately kept simple, is designed for application with information available solely from routine surface weather observations. It makes use of a very simple two-stream approximation and mean climatological reflection and transmission coefficients determined from the SOLMET (1977)<sup>59</sup> data tabulations.

Atwater and Ball (1978,1981)<sup>55,60</sup> have also proposed a simple model for the computation of radiation received at the ground based upon standard surface meteorological observations. It is believed that the model incorporates multiple reflections and the observed nonlinearities of reflectance, transmittance and absorptance with fractional cloud amounts in a more realistic fashion.

<sup>54</sup> Kasten, F. and G. Czeplak, 1980: Solar and terrestrial radiation dependent on the amount and type of cloud. *Solar Energy*, 24, 177-190.

<sup>55</sup> Atwater, M. A. and J. T. Ball, 1978: A numerical solar radiation model based on standard meteorological observations. *Solar Energy*, 21, 163-170.

<sup>56</sup> Tabata, S., 1964: Insolation in relation to cloud amount and sun's altitude. *Studies in Oceanography, Hidaka Volume*, 202-210.

<sup>57</sup> Lumb, F. E., 1964: The influence of cloud on hourly amounts of total solar radiation at the sea surface. *Quart. J. Roy. Meteor. Soc.*, 90, 43-56.

<sup>58</sup> Vowinckel, E. and S. Orvig, 1962: Relations between solar radiation and cloud type in the Arctic. *J. Appl. Meteor.*, 1, 552-559.

<sup>59</sup> SOLMET, 1977: Hourly solar radiation - surface meteorological observations. Vol. 1 - Users Manual. Vol. 2, 1979, Final Report. National Climatic Center, NOAA, EDIS, TD-9724.

<sup>60</sup> Atwater, M. A. and J. T. Ball, 1981: A surface solar radiation model for cloudy atmospheres. *Mon. Wea. Rev.*, 109, 878-888.

## 2. MODEL STRUCTURE

The model atmosphere is composed of  $n$ , plane-parallel homogeneous layers of arbitrary thickness. In addition, the ground surface constitutes another "layer" with the special property that its transmission is zero.

Of the radiation incident on layer  $k$ , the fractions reflected, transmitted and absorbed are given by  $R_k$ ,  $T_k$ , and  $A_k$ , respectively, where

$$R_k + T_k + A_k = 1. \quad (1)$$

For simplicity,  $R_k$ ,  $T_k$  and  $A_k$  are assumed not to depend upon the direction of the incident flux; that is, they are assumed to be the same for both upward and downward fluxes. However, as will be seen, some distinction is made between direct and diffuse radiation, and to the extent that the direct and diffuse radiative components depend upon the direction of the flux, so do the coefficients.

Another simplification implicit in Eq. (1) is that solar radiation may be treated as quasi-monochromatic. Selective absorption and scattering by gases and aerosols are treated in a crude fashion by the choice of values assigned to  $R_k$ ,  $T_k$ , and  $A_k$  for the various atmospheric layers.

In Figure 1, the horizontal lines numbered 1 through  $n$  represent  $n$  homogeneous atmospheric layers and  $g$  represents the ground surface.  $X_k$  represents the radiation impinging upon layer  $k+1$  from above and  $Y_k$  represents the upward-directed radiation emanating from layer  $k+1$ . Thus  $X_0$  is the amount of radiation from the sun reaching the top of the atmosphere vertically incident on a unit horizontal surface.  $Y_0$  is the amount of solar radiation reflected back to space by the earth-atmosphere system.  $X_n$ , the quantity in which we are particularly interested, is the solar radiation, both direct and diffuse, received at the ground. Each  $X_k$  and  $Y_k$  is composed of differing fractions of direct and diffuse radiation, and while it would be possible to take account of the direct and diffuse radiation separately, it is felt that this would needlessly complicate the procedure. Consequently, a simple but arbitrary distinction is made, which while crude, should account, at least in part, for the difference between the direct and diffuse components. All radiation is considered direct except for radiation transmitted through a layer containing at least 7/8 of any

1	↓ $X_0$	↑ $Y_0$
2	↓ $X_1$	↑ $Y_1$
3	↓ $X_2$	↑ $Y_2$
4	↓ $X_3$	↑ $Y_3$
...		
n	↓ $X_{n-1}$	↑ $Y_{n-1}$
g	↓ $X_n$	↑ $Y_n$

Figure 1. Flux of solar radiation through an atmosphere consisting of  $n$  homogeneous layers and a ground surface.

thick cloud. All radiation, once transmitted through such a cloud layer, is considered diffuse. All clouds, except for thin cirrus and cirrostratus, are considered thick.

The above system is described by  $2n+2$  linear equations for the  $2n+2$  fluxes ( $X_0, X_1, \dots, X_n; Y_0, Y_1, \dots, Y_n$ ) in terms of the specified coefficients  $R_k$  and  $T_k$ , ( $k = 0, 1, \dots, n$ ). The sequence of equations has the form

$$X_k = T_k X_{k-1} + R_k Y_k \quad (2)$$

$$Y_k = R_{k+1} X_k + T_{k+1} Y_{k+1} \quad (3)$$

where, of course,  $T_0 = 1$ ,  $R_0 = 0$ ,  $R_{n+1} = R_g$ , and  $T_{n+1} = T_g = 0$ .

Eq. (2) states that the downward flux of radiation leaving any layer  $k$  is equal to the fractional transmission of that layer ( $T_k$ ) times the downward flux of radiation reaching that layer from above ( $X_{k-1}$ ) plus the fractional reflection of that layer ( $R_k$ ) times the upward flux of radiation reaching that layer from below ( $Y_k$ ). Eq. (3) makes comparable statements about the upward-directed flux.

The absorption of solar radiation in any layer  $k$  is obtained from Eqs. (2) and (3) and is given by

$$S_k = X_{k-1} + Y_k - X_k - Y_{k-1} \quad (4)$$

and the total amount of energy absorbed in the atmosphere is

$$S = \sum_{k=1}^n S_k = X_0 - Y_0 - (1 - R_g) X_n. \quad (5)$$

The system of Eqs. (2) and (3) can be solved for any of the fluxes in terms of specified values for the reflection and transmission coefficients. In general, such solutions require the inversion of a  $(2n+2)$  square matrix, a not inconsiderable task for even moderately large values of  $n$ . Fortunately, because the matrix contains only a limited number of non-zero elements, it was possible to find closed form solutions for  $Y_0$  and  $X_n$ , for any  $n$ . This implies closed form solutions for all of the fluxes, since they can be obtained directly by a simple stepwise process from the system of Eqs. (2) and (3) once a solution for  $Y_0$  or  $X_n$  is known. The solu-

tions for  $Y_0$  and  $X_n$  are:

$$Y_0 = X_0 \begin{bmatrix} R_1 + R_2 T_1^2 D_0^{-1} + R_3 (T_1 T_2)^2 (D_0 D_1)^{-1} + \\ + R_4 (T_1 T_2 T_3)^2 (D_1 D_2)^{-1} + \dots + \\ + R_n (T_1 T_2 \dots T_{n-1})^2 (D_{n-3} D_{n-2})^{-1} + \\ + R_n (T_1 T_2 \dots T_n)^2 (D_{n-2} D_{n-1})^{-1} \end{bmatrix} \quad (6)$$

$$X_n = T_1 T_2 \dots T_n X_0 / D_{n-1} \quad (7)$$

where

$$D_0 = d_1$$

$$D_1 = d_2 D_0 - R_1 R_3 T_2^2$$

$$D_2 = d_3 D_1 - D_0 R_2 R_4 T_3^2 - R_1 R_4 (T_2 T_3)^2$$

$$D_3 = d_4 D_2 - D_1 R_3 R_5 T_4^2 - D_0 R_2 R_5 (T_3 T_4)^2 - R_1 R_5 (T_2 T_3 T_4)^2$$

$$\vdots$$

$$D_{n-1} = d_n D_{n-2} - D_{n-3} R_{n-1} R_{n+1} T_n^2 - D_{n-4} R_{n-2} R_{n+1} (T_{n-1} T_n)^2 -$$

$$- D_{n-5} R_{n-3} R_{n+1} (T_{n-2} T_{n-1} T_n)^2 - \dots -$$

$$- D_0 R_2 R_{n+1} (T_3 T_4 \dots T_n)^2 - R_1 R_{n+1} (T_2 T_3 \dots T_n)^2$$

and

$$d_1 = 1 - R_1 R_2$$

$$d_2 = 1 - R_2 R_3$$

.

.

.

$$d_n = 1 - R_n R_{n+1}.$$

The particular solutions of interest in the present application are for  $n = 3$ . This is the simplest geometry that makes use of the standard cloud code information which categorizes clouds into high, middle, and low cloud types. These solutions are:

$$Y_0 = \left[ R_1 + R_2 T_1^2 D_0^{-1} + R_3 (T_1 T_2)^2 (D_0 D_1)^{-1} + R_g (T_1 T_2 T_3)^2 (D_1 D_2)^{-1} \right] X_0 \quad (8)$$

$$X_3 = T_1 T_2 T_3 X_0 / D_2 \quad (9)$$

where

$$D_0 = d_1 = 1 - R_1 R_2$$

$$D_1 = d_1 d_2 - R_1 R_3 T_2^2 = (1 - R_1 R_2)(1 - R_2 R_3) - R_1 R_3 T_2^2$$

$$D_2 = d_3(d_1 d_2 - R_1 R_3 T_2^2) - d_1 R_2 R_g T_3^2 - R_1 R_g (T_2 T_3)^2$$

$$- 1 - (R_1 R_2 + R_2 R_3 + R_3 R_g) - (R_1 R_3 T_2^2 + R_2 R_g T_3^2 + R_1 R_g T_2^2 T_3^2)$$

$$+ (R_1 R_2^2 R_3 + R_2 R_3^2 R_g + R_1 R_2 R_3 R_g + R_1 R_3^2 R_g T_2^2 + R_1 R_2^2 R_g T_3^2)$$

$$- R_1 R_2^2 R_3^2 R_g.$$

It is interesting to note that the solution for  $Y_0$  is expressed as a sum of terms, each of which contains the contribution from a separate layer. The interactions among the various layers for both  $Y_0$  and  $X_n$  are contained in the expressions for  $D_0$ ,  $D_1$  and  $D_2$ .

As an aid in the visualization of the meaning of the solutions, Figure 2 traces each individual component of the radiative fluxes for a 3-layer atmosphere in which the ground surface reflectivity  $R_g = 0$ . In this case Eqs. (8) and (9) are simplified, since in addition to removing the term containing  $R_g$  in Eq. (8),  $D_2$  in Eqs. (8) and (9) reduces to  $D_1$ .

Figure 2 starts with the extra-terrestrial radiation  $X_0$  impinging on the top of layer 1. Part of this radiation ( $R_1 X_0$ ) is immediately reflected back to space and part ( $T_1 X_0$ ) is transmitted to layer 2. Part of the latter component is transmitted to layer 3 ( $T_1 T_2 X_0$ ) and part reflected up to

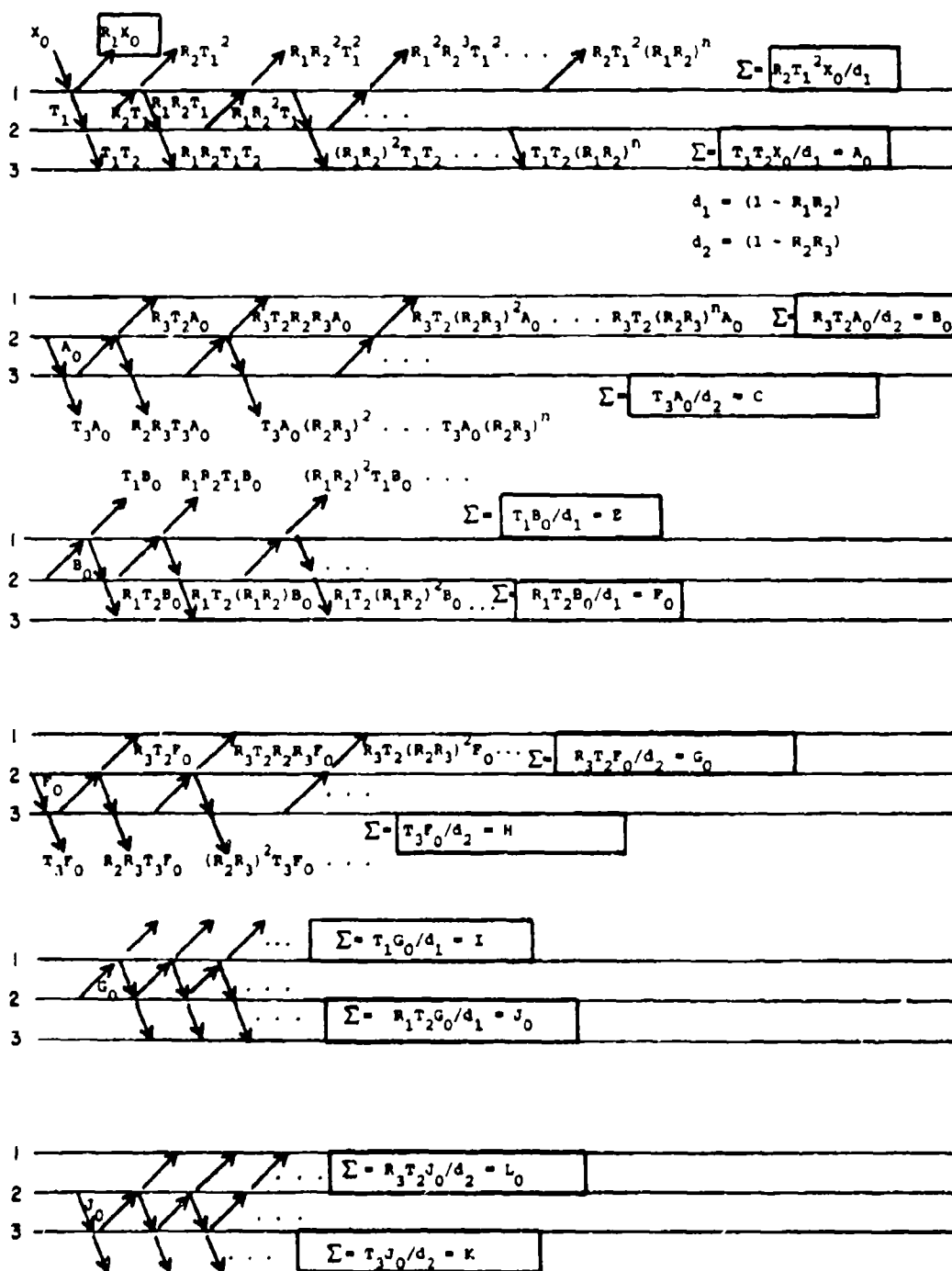


Figure 2. Schematic accounting of the flux of solar radiation through a 3-layer atmosphere above a black ground surface.

the bottom of layer 1 ( $R_2 T_1 X_0$ ). Part of this latter component ( $R_2 T_1^2 X_0$ ) is transmitted through layer 1 to space and part ( $R_1 R_2 T_1 X_0$ ) is returned to the top of layer 2. This returned component is  $R_1 R_2$  times the component ( $T_1 X_0$ ) which had previously been transmitted to the top of layer 2. Therefore, the next component transmitted to space is  $R_1 R_2$  times the antecedent component; namely,  $R_1 R_2^2 T_1^2 X_0$ . The next component transmitted to space arising from the earlier  $T_1 X_0$  component and each following component is  $R_1 R_2$  times its antecedent component. This infinite series is a geometric progression,  $R_2 T_1^2 X_0 + R_1 R_2^2 T_1^2 X_0 + R_1^2 R_2^3 T_1^2 X_0 + \dots$ , whose sum is  $R_2 T_1^2 X_0 / d_1$ . Similarly, an infinite series of flux terms emanating from  $T_1 X_0$  is transmitted down through layer 2 to the top of layer 3. This series also forms a geometric progression ( $T_1 T_2 X_0 + R_1 R_2 T_1 T_2 X_0 + [R_1 R_2]^2 T_1 T_2 X_0 + \dots + [R_1 R_2]^p T_1 T_2 X_0$ ) whose sum, as  $p$  approaches infinity, is  $T_1 T_2 X_0 / d_1$ , which is labeled  $A_0$  for convenience.

The second row of Figure 2 starts with  $A_0$ , the sum of the radiative flux emanating from  $T_1 X_0$  and reaching layer 3 from above, and traces the progress of this radiation as part of it is transmitted through layer 3 to the ground, where it is absorbed and part of it is transmitted up through layer 2 to the bottom of layer 1. These components form additional infinite series whose sums are  $T_3 A_0 / d_2 = C$  for the radiation reaching the ground and  $R_3 T_2 A_0 / d_2 = B_0$  for the radiation transmitted up to layer 1.

Again, starting with  $B_0$ , another pair of infinite series of components is formed. The sum of the series consisting of the radiation transmitted to space is  $T_1 B_0 / d_1 = E$ , and the sum of the series consisting of the radiation transmitted down through layer 2 to the top of layer 3 is  $R_1 T_2 B_0 / d_1 = F_0$ . From  $F_0$  another pair of infinite series is formed. The sum of the terms transmitted through layer 3 to the ground is  $T_3 F_0 / d_2 = H$  and the sum of the terms transmitted through layer 2 up to the bottom of layer 1 is  $R_3 T_2 F_0 / d_2 = G_0$ .  $G_0$  forms a pair of infinite sums,  $T_1 G_0 / d_1 = I$  (out to space) and  $R_1 T_2 G_0 / d_1 = J_0$  (down to the top of layer 3).  $J_0$  forms a pair of infinite series,  $T_3 J_0 / d_2 = K$  (down to the ground), and  $R_3 T_2 J_0 / d_2 = L_0$  (up to the bottom of layer 1). It is apparent that this process of formation of a pair of infinite sums from each previous infinite sum continues indefinitely.

If we add the infinite sums reaching the ground, we have



$$X_3 = C + H + K + \dots$$

where

$$C = T_3 A_0 / d_2 = T_1 T_2 T_3 X_0 / d_1 d_2$$

$$H = T_3 T_0 / d_2 = R_1 T_2 T_3 B_0 / d_1 d_2 = R_1 R_3 T_2^2 T_3 A_0 / d_1 d_2^2$$

$$= R_1 R_3 T_1 T_2^3 T_3 X_0 / (d_1 d_2)^2, \text{ and}$$

$$K = T_3 J_0 / d_2 = R_1 T_2 T_3 G_0 / d_1 d_2 = R_1 R_3 T_2^2 T_3 F_0 / d_1 d_2^2$$

$$= R_1^2 R_3 T_2^3 T_3 B_0 / (d_1 d_2)^2 = R_1^2 R_3^2 T_2^4 T_3 A_0 / d_1^2 d_2^3$$

$$= R_1^2 R_3^2 T_1 T_2^5 T_3 X_0 / (d_1 d_2)^3.$$

C, H, K, . . . are each the sums of infinite series, but their sum ( $X_3$ ) is an infinite series of infinite sums, whose sum is given by

$$C + H + K + \dots = \frac{T_1 T_2 T_3 X_0}{d_1 d_2} (1 + R_1 R_3 T_2^2 / d_1 d_2 + (R_1 R_3)^2 T_2^4 / (d_1 d_2)^2 + \dots)$$

$$= \frac{T_1 T_2 T_3 X_0}{d_1 d_2} \left( \frac{1}{1 - R_1 R_3 T_2^2 / d_1 d_2} \right)$$

$$= \frac{T_1 T_2 T_3 X_0}{d_1 d_2 - R_1 R_3 T_2^2} = X_3$$

which is what is obtained from Eq. (9) when  $R_q = 0$ .

Similarly,  $Y_0$  is an infinite sum of infinite sums such that,

$$Y_0 = R_1 X_0 + R_2 T_1^2 X_0 / d_1 + E + I + \dots$$

where  $E = T_1 B_0 / d_1 = R_3 T_1 T_2 A_0 / d_1 d_2 = R_3 (T_1 T_2)^2 X_0 / d_1^2 d_2$  and

$$I = T_1 G_0 / d_1 = R_3 T_1 T_2 F_0 / d_1 d_2 = R_1 R_3 T_1 T_2^2 B_0 / d_1^2 d_2$$

$$= R_1 R_3^2 T_1 T_2^3 A_0 / (d_1 d_2)^2 = R_1 R_3^2 T_1^2 T_2^4 X_0 / d_1^3 d_2^2$$

and where

$E + I + \dots$  form the series

$$\begin{aligned}
E + I + \dots &= \frac{R_3 (T_1 T_2)^2 X_0}{d_1^2 d_2} \left( 1 + \frac{R_1 R_3 T_2^2}{d_1 d_2} + \frac{(R_1 R_3)^2 T_2^4}{(d_1 d_2)^2} + \dots \right) \\
&= \frac{R_3 (T_1 T_2)^2 X_0}{d_1^2 d_2} \left( \frac{1}{1 - \frac{R_1 R_3 T_2^2}{d_1 d_2}} \right) = \frac{R_3 (T_1 T_2)^2 X_0}{d_1^2 d_2} \left( \frac{d_1 d_2}{d_1 d_2 - R_1 R_3 T_2^2} \right) \\
&= \frac{R_3 (T_1 T_2)^2 X_0}{d_1 (d_1 d_2 - R_1 R_3 T_2^2)}. \quad \text{Thus}
\end{aligned}$$

$$Y_0 = X_0 \left[ R_1 + \frac{R_2 T_1^2}{d_1} + \frac{R_3 (T_1 T_2)^2}{d_1 (d_1 d_2 - R_1 R_3 T_2^2)} \right]$$

which is what is obtained from Eq. (8) when  $R_q = 0$ .

### 3. REFLECTIVITY, TRANSMISSIVITY AND ABSORPTIVITY COEFFICIENTS

It is apparent that the main impediment to the immediate application of the model is a lack of information on appropriate values of the reflectivity, transmissivity and absorptivity ( $R$ ,  $T$ ,  $A$ ) coefficients. These coefficients are not constants but are functions of space and time. We cannot expect to account for all of the variability, but much if not most of the variability is a function of cloud amount and type. The solar zenith angle is another important source of variability. These sources can easily be incorporated from routine observations.

If the individual layers are thin enough,  $R$ ,  $T$ , and  $A$  for any particular layer can be treated as a constant for that layer, time, and location. It is not possible to specify how many layers the atmosphere should be divided into in order to justify the above assumption, but it would undoubtedly be more than the three layers we will be using for our first approximation.

Although some effort has been made to measure R, T and A directly, as indicated in the Introduction, such measurements are difficult and expensive. Therefore, too few cloud types, for relatively few varieties of conditions, have been measured to permit confidence in the results. Furthermore, measurements for the same cloud type show large variations. Part of the variability is due to the natural variability in cloud microphysics for the same cloud type from time to time and from place to place. However, other sources of variability almost invariably contaminate the results. These include variations in the reflectivity of the surface (either ground or cloud) underlying the cloud layer being measured as well as instrumental errors. Furthermore, measurement of any (R, T, A) coefficient, such as  $R_{k+1}$ , the reflectivity of layer k+1, involves more than the relatively simple measurement of  $Y_k/X_k$ , the albedo of layer (k+1).

We have from Eq. (3)

$$R_{k+1} = \frac{Y_k}{X_k} - \frac{T_{k+1}Y_{k+1}}{X_k} \quad (10)$$

This means that  $Y_{k+1}$ , the upward radiation at the bottom of layer k+1, must also be measured simultaneously and there must be knowledge of the transmissivity of the cloud ( $T_{k+1}$ ). But from Eq. (2) we have

$$T_{k+1} = \frac{X_{k+1}}{X_k} - \frac{R_{k+1}Y_{k+1}}{X_k} \quad (11)$$

This means that one cannot simply measure  $R_{k+1}$  and  $T_{k+1}$  separately, but that both must be measured simultaneously, which means that four flux terms  $X_k$ ,  $Y_k$ ,  $X_{k+1}$ , and  $Y_{k+1}$  must be measured simultaneously. However, experiments designed to measure cloud reflectivity typically measure simultaneously only the downward and upward directed fluxes above the cloud layer. Furthermore, aircraft measurements suffer from the difficulties inherent in the instability of the platform.

If layer (k+1) is a thick undercast layer situated above a relatively low-albedo surface, then both the  $T_{k+1}$  and  $Y_{k+1}$  will be small and the fraction  $Y_k/X_k$  will closely approximate  $R_{k+1}$ . However, if the cloud undercast is thin or has thin spots or is situated above a relatively high-albedo surface, then  $Y_k/X_k$  may be a poor approximation of  $R_{k+1}$ . Furthermore, the

measurements are likely to suffer from large variability under such circumstances.

Because of the incomplete and unreliable nature of the direct measurements, we have obtained the (R, T, A) coefficients indirectly using the SOLMET (1977) data base. The construction of the SOLMET data base was undertaken by the National Climatic Center with support from the Department of Energy. It involved the rehabilitation of the historical hourly solar radiation data for 26 National Weather Service stations and the incorporation of these data along with the standard hourly meteorological surface observations for these stations into a standard format on computer tape. The raw hourly global irradiance data from Eppley bulb-type pyranometers contained calibration errors and changes in radiation scale and suffered from decolorization of the black coating (Hoyt, 1979)<sup>61</sup>. A goal of the rehabilitation was to provide a homogeneous, consistent set of data with at most a 5 percent error. There may be some question whether this goal was reached (Hoyt, 1979) but it was at least approached. Nevertheless, because of the large amount of data, random errors should be virtually absent from mean values. Therefore it was felt that mean values of global irradiance for specified sky states and zenith angles would be reliable. The observed irradiance data are equivalent to  $X_3$  in the 3-layer model.

We made use of observed mean values of  $X_3$  for specified conditions to obtain the (R, T, A) coefficients for each of the three layers. In essence we inverted the model solutions ( $\hat{X}_3$ ) in order to obtain the (R, T, A) coefficients. In doing this we have worked primarily with uniform sky states; that is, where all three layers are clear or where the first layer observable from the ground is overcast. In the case of clear skies or high clouds there is no ambiguity; however, in the case of middle or low layer overcast we have no knowledge of the presence or absence of higher clouds. This uncertainty contributes to some dispersion in the results for middle and low clouds, but the final (R, T, A) coefficients which are obtained reflect climatological mean conditions. Thus, we do not claim that the coefficients obtained, say, for some low cloud type, represent the characteristics of that type, but rather that they reflect the characteristics of that type modified by the climatology of middle and high clouds associated with

---

<sup>61</sup> Hoyt, D. V., 1979: An error in the rehabilitation of the National Weather Service solar radiation data. *Solar Energy*, 23, 557-559.

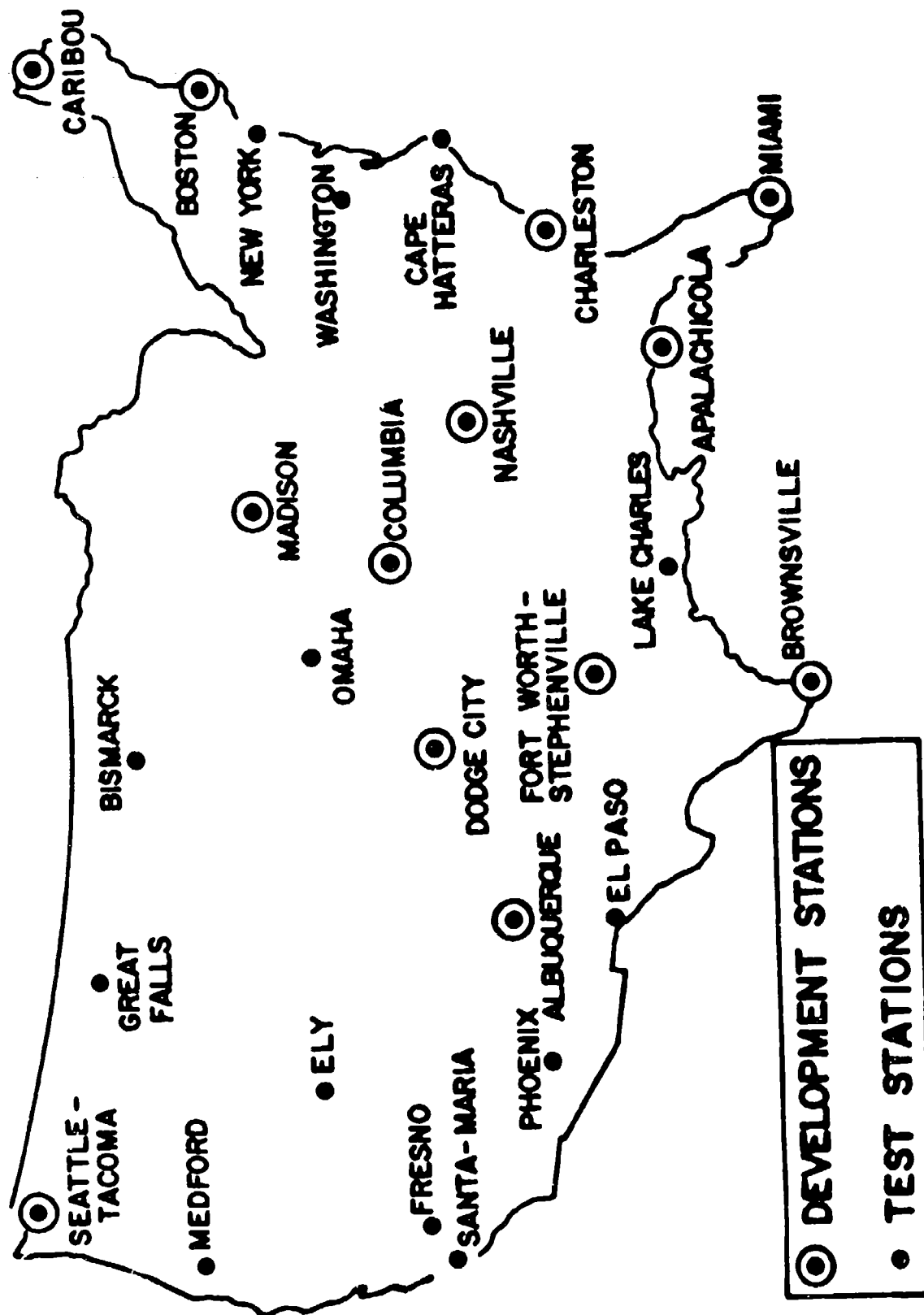
that type. It will become apparent that this source of error is a relatively minor consideration.

Table 1 summarizes the observed data for the 13 stations designated in Figure 3 as the development stations. The data are given as a function of certain uniform sky/weather states and the cosine of the zenith angle,  $\cos z$ . The transmission of solar radiation to the ground is expressed as 1000 times the average fraction of the extra-terrestrial radiation ( $X_0$ ). The  $\cos z$  intervals range  $\pm 0.05$  from the designated central values. Although nine different cloud types are recognized by the standard synoptic code at each of the three cloud levels, many of these cloud types are rare. Nine cloud types occur with sufficient frequency to obtain reliable mean values. These are thin and thick cirrus (Ci), thin and thick cirrostratus (Cs), altostratus (As), altocumulus (Ac), cumulus (Cu), stratocumulus (Sc), and stratus (St). The mean values of  $X_3$  observed with certain cloud types were indistinguishable from each other. Therefore, in Table 1 Ci and Cs are combined into a single high cloud type (Ci/Cs), As and Ac are combined into a single middle cloud type (As/Ac), and low clouds Sc and St are also combined. There is however a large difference between thin and thick Ci/Cs relevant to the observed mean values of  $X_3$ .

In addition to cloud types and clear skies, Table 1 contains some weather categories. A small but distinct difference was found between values of  $X_3$  for cases where fog or smoke or both (F/K) were reported and those cases in which no present weather was reported for the categories of clear skies or high overcast. For the remaining cloud categories no appreciable difference was discernible. Consequently separate (R, T, A) coefficients were obtained for (F/K) only for the categories of clear and high overcast. The last row in Table 1 contains mean values of  $X_3$  for those cases in which any kind of precipitation is reported. The mean values associated with precipitation are the least reliable. This is partly due to the smaller number of cases and partly due to the fact that these values represent weighted means of several different cloud types. Each of the cloud types may have somewhat different radiation characteristics. Therefore, with the same individual mean values for each cloud type, different distributions of cloud types will yield different observed values for the fractional transmission.

# SOLMET STATION NETWORK

Figure 3.



The weighted average of the standard deviations associated with the values of Table 1 is 0.087. While there is no consistent variation with zenith angle, there is a pronounced variation with sky condition. The average standard deviations vary by about a factor of two from 0.067 for clear skies to 0.132 for overcast low clouds.

TABLE 1. OBSERVED AVERAGE FRACTIONAL TRANSMISSION TO THE GROUND (X 1000) FOR 13 DEVELOPMENT STATIONS. CLOUD VALUES REPRESENT OVERCAST CONDITIONS.

	COS Z									
	.05	.15	.25	.35	.45	.55	.65	.75	.85	.95
CLEAR	460	512	619	685	735	770	783	792	794	794
CLEAR (F/K)	390	427	520	602	655	688	704	715	720	722
THIN Ci/Cs	395	436	526	602	660	692	712	729	733	736
THIN Ci/Cs (F/K)	338	367	446	532	591	621	642	660	666	671
THICK Ci/Cs	284	319	396	452	508	550	573	595	604	604
THICK Ci/Cs (F/K)	257	289	357	407	456	493	513	533	540	540
Cu/Cb	150	179	220	260	290	316	335	350	365	380
As/Ac	184	204	244	271	297	315	325	335	338	338
Sc/St	117	139	178	208	232	250	266	280	290	296
PRECIPITATION	095	105	123	135	146	154	158	161	162	162

It is apparent that  $X_3$  is appreciably smaller when there is precipitation, especially for large values of  $\cos z$ . Since it is unlikely that the precipitation itself has such a large effect on the transmission of solar radiation, it was assumed for purposes of calculation that when precipitation is occurring there are overcast clouds in all three layers: thick Ci/Cs, As/Ac, and Sc/St. However, when there is no precipitation the sky is assumed to be clear above the lowest overcast layer. Thus the reflectivity and absorptivity coefficients for middle and low layer overcast are undoubtedly biased toward higher values.

The results in Table 1 were obtained separately for each of the 13 stations and for each month in order to accommodate possible geographical or seasonal variations. However, since no clear geographical or seasonal differences could be discerned, the separate results were combined. Presumably, if the data were less noisy some small, but real geographical and seasonal differences might have been uncovered. The data were also examined separately for hours before and after noon, but here, too, no systematic differences were found.

The values of Table 1 are shown graphically in Figure 4, where it is

possible to discern more clearly the variation with  $\cos z$ . It is also clear from Figure 4 that little insolation reaches the ground when precipitation is occurring and that this insolation varies little with  $\cos z$ . It is interesting to note, for  $\cos z > 0.5$ , that while the differences are small, the transmission for overcast Cu/Cb is greater than that for overcast As/Ac. On the other hand, for  $\cos z < 0.5$ , the reverse is true. A possible interpretation of this result is that Cu/Cb are convective clouds with appreciable vertical development. Therefore, even when the layer is overcast, there are likely to be small breaks or thin spots in the cloud layer. When the sun is high in the sky some solar radiation may reach the ground relatively unimpeded, but because of the vertical cloud development, more radiation is likely to be blocked by cloud sides when  $\cos z < 0.5$ .

(R, T, A) coefficients evaluated for clear skies and for the various overcast cloud layers are presented in Tables 2 and 3. The evaluation process was a stepwise procedure which started with the simplest and least ambiguous sky state and advanced in stages to the most complex state. Since it was our intention to treat solar radiation as monochromatic and to determine a single set of clear layer coefficients, processes such as ozone and water vapor absorption, molecular scattering, and scattering and absorption by aerosols could be incorporated in only the most rudimentary fashion. Since the largest effect on insolation is due to clouds and since we are approximating the atmosphere with only 3 layers, a more sophisticated treatment of the clear layers was deemed unwarranted.

TABLE 2. ESTIMATES OF REFLECTIVITIES, TRANSMISSIVITIES AND ABSORPTIVITIES (X 1000) FOR CLEAR SKY LAYERS.

	COS Z										D
	.05	.15	.25	.35	.45	.55	.65	.75	.85	.95	
R1	104	088	057	042	033	028	026	024	024	024	
R2	130	112	077	056	046	039	036	034	034	034	040
R3	135	117	078	060	051	045	042	040	040	040	045
R3 (F/K)	244	231	189	147	127	116	110	105	102	100	116
T1	799	823	869	896	915	927	932	936	937	937	
T2	733	767	829	865	889	906	912	916	917	917	905
T3	728	762	828	861	884	900	906	909	910	910	900
T3 (F/K)	598	616	677	743	776	794	804	811	815	818	788
A1	097	089	074	062	052	045	042	040	039	039	
A2	137	121	094	079	065	055	052	050	049	049	055
A3	137	121	094	079	065	055	052	051	050	050	055
A3 (F/K)	158	153	134	110	097	090	086	084	083	082	096



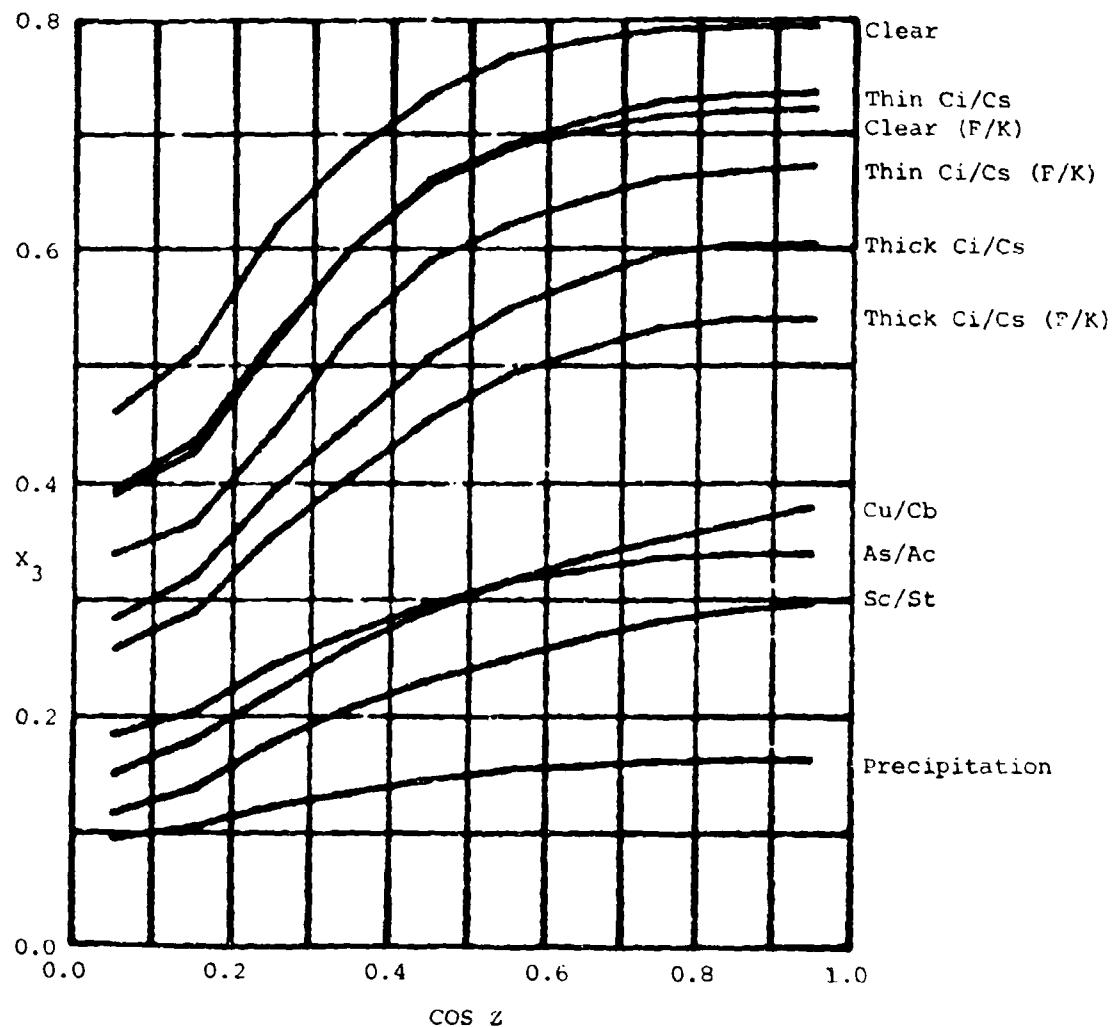


Figure 4. Observed fractional transmission to ground for development stations.

TABLE 3. ESTIMATES OF REFLECTIVITIES, TRANSMISSIVITIES AND ABSORPTIVITIES  
(X 1000) FOR OVERCAST CLOUD LAYERS.

	COS Z										D
	.05	.15	.25	.35	.45	.55	.65	.75	.85	.95	
THIN Ci/Cs (R1)	240	235	211	170	143	134	120	106	103	100	
THICK Ci/Cs (R1)	568	535	460	401	342	297	273	249	240	240	
As/Ac (R2)	650	645	621	604	587	576	569	562	560	560	560
Cu/Cb (R3)	661	650	636	611	592	575	561	549	535	520	520
Sc/St (R3)	703	693	676	660	648	639	629	620	613	609	609
THIN Ci/Cs (T1)	663	676	715	768	805	817	833	849	853	857	
THICK Ci/Cs (T1)	309	350	440	508	578	631	660	689	700	700	
As/Ac (T2)	211	230	268	292	317	333	343	353	356	356	361
Cu/Cb (T3)	199	226	254	287	310	331	349	363	379	395	400
Sc/St (T3)	153	173	203	227	245	258	273	286	296	302	311
THIN Ci/Cs (C1)	000	000	000	000	000	004	005	005	005	004	
THICK Ci/Cs (C2)	026	026	026	029	028	027	025	022	021	021	
As/Ac (C3)	002	004	017	025	031	036	036	035	035	035	024
Cu/Cb (C3)	003	003	016	023	033	039	038	037	036	035	025
Sc/St (C3)	007	013	027	034	042	048	046	043	041	039	025

We assume that the reflectivity, transmissivity and absorptivity are modeled by

$$R_k = \phi_k \rho_k + (1 - \phi_k) r_k \quad (12)$$

$$T_k = \phi_k \tau_k + (1 - \phi_k) t_k \quad (13)$$

$$A_k = a_k + c_k \quad (14)$$

where  $r_k$ ,  $t_k$ , and  $a_k$  are the corresponding coefficients for clear layers and  $\rho_k$  and  $\tau_k$  are the reflectivities and transmissivities for overcast cloud layers.  $c_k$  is a small correction added to the clear layer absorption to account for absorption by liquid water when layer  $k$  is overcast.  $r_k$ ,  $t_k$ , and  $a_k$  are functions of  $\cos z$  as well as  $k$ .  $\rho_k$ ,  $\tau_k$ , and  $c_k$  are, in addition, functions of cloud type.  $\phi_k$  is a weighting function which depends upon fractional cloud cover. A full discussion of  $\phi_k$  will be given, but for the present it is sufficient to indicate that  $\phi_k = 0$  when layer  $k$  is clear and  $\phi_k = 1$  when layer  $k$  is overcast.

We assigned tentative values for the reflectivity ( $r_k$ ) and absorptivity ( $a_k$ ) for each of the three clear layers based upon the mass contained in

each layer, modified so as to include in a crude fashion ozone and water vapor absorption and scattering and absorption by aerosols. Care was taken to remain consistent with available information on these clear layer characteristics. The clear layer transmissivities were then obtained from Eq. (1),

$$t_k = 1 - r_k - a_k = 1 - R_k - A_k = T_k.$$

It can be seen from Eq. (9) that  $X_3$  depends upon the ground albedo ( $R_g$ ) in addition to the (R, T) coefficients for the 3 layers. The SOLMET data unfortunately do not contain specific information on ground albedo. We therefore used a climatological mean value of 0.15 for  $R_g$  throughout this study, rather than attempt to estimate  $R_g$  as a function of time and location. In practice, however, specific information on the state of the ground will permit the use of a more suitable value.

$\hat{X}_3$  was calculated using the tentative values of  $R_k$  and  $T_k$  for the clear sky layers and the assumed value of  $R_g$ . Relatively minor adjustments were made in  $R_k$  and  $T_k$  as necessary, in order to ensure that  $\hat{X}_3$  matched the observed mean values of  $X_3$  for each  $\cos z$  category. These values were approximately the same as those contained in the first 3 rows of each part of Table 2. They were not identical because  $R_k$  and  $T_k$  for the atmospheric layers are not uniquely determined by  $X_3$ . Thus it was necessary, as the coefficients for cloud types were evaluated, to make further adjustments in the coefficients already determined. However, in all cases the required adjustments were of a minor nature.

Using a similar procedure, separate coefficients,  $R_3(F/K)$  and  $T_3(F/K)$ , were determined for the bottom layer for those clear sky situations in which fog or smoke or fog and smoke were reported as obstructions to visibility, but where the sky is not obscured. Situations in which the sky is obscured are treated as a stratus overcast if the obscuration is fog or as a precipitation case if precipitation is the source of the obscuration.

The presence of smoke or fog was assumed limited to the lowest layer. Therefore in evaluating  $\hat{X}_3$  for clear skies where smoke or fog is reported, the same values of  $R_k$  and  $T_k$  are used for  $k = 1$  and  $2$  as when no obstructions to visibility are present.

The next stage in the process was to evaluate  $R_k$  and  $T_k$  for the var-

ious uniform cloud layers. The general procedure was to start with the simplest and least ambiguous cases, that is, with thin Ci/Cs overcast, and advance to increasingly complex states. As in the clear sky cases, we used available data (in this case cloud reflectivity observations) as a first approximation. We made the minor additions indicated in the bottom section of Table 3 for absorption by clouds ( $c_k$ ) and determined  $T_k$  from Eq. (1). In the process of matching  $\hat{X}_3$  to the observed mean values of  $X_3$  to obtain the coefficients for, say, thin Ci/Cs overcast, only the coefficients for the top layer (layer 1) are affected by the presence of clouds, since the only clouds in this group of cases are high thin overcast clouds. The coefficients for layers 2 and 3 are the appropriate clear sky values from Table 2. After we determined the tentative coefficients for thin Ci/Cs, we tested them by comparing  $\hat{X}_3$  and  $X_3$  for those situations where the only clouds present are thin Ci/Cs and where smoke and/or fog are reported as obstructions to visibility. These latter cases were not used in obtaining the tentative coefficients for this Ci/Cs, but since the presence of F/K only affects layer 3, some adjustments in coefficients were necessary so that the observed mean values of  $X_3$  are matched by calculated values ( $\hat{X}_3$ ) whether or not smoke and/or fog is present. Inasmuch as  $R_3$  and  $T_3$  are appreciably different when smoke and/or fog are present, the requirement for matching both situations imposes severe restrictions on freedom of choice for  $R_1$  and  $T_1$  for thin Ci/Cs overcast. After final values for thin Ci/Cs were determined, the process of coefficient evaluation was repeated for thick Ci/Cs, including the requirement for matching calculated and observed values of insolation for both the presence and absence of obstructions to visibility.

The next stage was the evaluation of coefficients for middle layer overcast (As/Ac). The same process as above was followed, except for the part concerned with (F/K), since the observed values of  $X_3$  were not noticeably dependent on the presence or absence of obstructions to visibility when middle or low overcast was present. It can be seen from Table 3 that the variation of middle layer coefficients with  $\cos z$  is much smaller than that of the high layer clouds. This is obviously due to the greater thickness or density of middle clouds. It will be seen that the coefficients for low clouds also have a relatively small variation with  $\cos z$ .

In Tables 2 and 3, the coefficients for the middle and low layers have additional values in a column labeled D. This column refers to diffuse radiation coefficients which do not depend upon  $\cos z$ . Distinction should properly be made between direct and diffuse radiation in all three layers. However, to do so in a precise fashion would introduce a major complication in the calculations. Therefore, as indicated previously, we assume that all radiative fluxes are direct except for radiation below an overcast or nearly overcast (cloud fraction  $\geq 7/8$ ) thick cloud layer, where we assume that all radiative fluxes are diffuse. Thus, constant values (column D) are used for both layers 2 and 3 regardless of the value of  $\cos z$  when there is  $7/8$  or more of thick Ci/Cs. If the thick cloud is situated in layer 2, then diffuse coefficients are used only for layer 3.

Clear-layer D-values (Table 2) are used for  $R_2$  and  $T_2$  when there is a thick Ci/Cs overcast and layer 2 is clear. Similarly, in layer 3, clear-layer D-values are used when there is either a middle layer overcast or a high thick overcast. However, with regard to layer 3, there is a choice to be made for the appropriate clear-layer D values; namely,  $R_3$  and  $T_3$  or  $R_3(F/K)$  and  $T_3(F/K)$ . The latter are used when smoke and/or fog are reported and the thick overcast is a high cloud. The former are used when no obstructions to visibility are present, or regardless of the presence or absence of obscurations to visibility, when the thick overcast is a middle cloud. This choice is consistent with the observation, already noted, that the insolation received at the ground in the presence of middle or low cloud overcast is approximately the same whether or not obstructions to visibility are reported.

Overcast-layer D-values (Table 3) are required for layers 2 and 3 when precipitation is reported since it is assumed that under this circumstance, thick overcast cloud layers are present in all 3 layers. Furthermore, overcast-layer D-values are used in layer 2 and/or layer 3 when the middle and/or low cloud cover is partial and is beneath a thick, higher-layer overcast. The insolation calculation for partial cloud cover will be discussed below.

The D-values in Tables 2 and 3 were chosen on the basis of the increased path-length appropriate for diffuse radiation as compared with a unit path-length for direct radiation ( $\cos z = 1.00$ ). The D-values were

obtained from the direct radiation values by interpolating for  $\cos z = 0.60$ , which yields a path-length equivalent to 1.66 times the unit path-length. Some minor adjustments were necessary for the clear sky D-values in order to match the calculated with the observed values of  $X_3$ . The overcast-layer D-values were also adjusted so as to improve the agreement between the computed and observed values of  $X_3$  for the precipitation cases.

The final stage in the selection of (R, T, A) coefficients was reserved for the low cloud-layer overcasts. Although the differences are observed to be small, a proper distinction can be made between the convective clouds (primarily cumulus, but including some cumulonimbus) and the layered clouds (stratus and stratocumulus) of layer 3. The values of the (R, T, A) coefficients in Table 3 are consistent with the available measurements for these cloud types and, what is probably more important, yield calculated values,  $\hat{X}_3$ , which match the observations in Table 1 in every  $\cos z$  category and every sky state except precipitation. While it would no doubt be possible to match the observations with different sets of coefficients, it is unlikely that it would be possible to do so with appreciably different coefficients which at the same time satisfy the various internal and physical constraints which were imposed. We reiterate, however, that the coefficients represent typical, temperate latitude average values in which a multitude of details is either suppressed or treated only approximately. Furthermore, only the high overcast cloud layer coefficients are unambiguous. The coefficients for middle and low clouds, when no precipitation is reported, are evaluated with the assumption that there are no clouds above the lowest overcast layer. This means that the reflectivity and absorptivity coefficients for the middle and low cloud types are probably somewhat too high and the transmissivity coefficients probably somewhat too low. However, this bias cannot exceed 5 to 10 percent since, for example, the reported measurements for middle and low cloud types average almost precisely the same as the average values indicated in Table 3.

The greatest uncertainty with respect to the (R, T, A) coefficients obtains with the diffuse coefficients for overcast middle and low clouds. Although there is a physical basis, their choice is essentially arbitrary. Furthermore, the manner in which these coefficients are used in the model to represent the flux of diffuse radiation is at best a crude approximation to the real atmosphere.

#### 4. WEIGHTING FUNCTION FOR FRACTIONAL CLOUD COVER

In order to compute the fraction of the extra-terrestrial radiation transmitted to the ground for the 3-layer atmosphere (Eq. 9) it is necessary to have values of  $R_k$  and  $T_k$  ( $k = 1, 2, 3$ ) as well as  $R_g$ , the ground albedo.  $R_g$  is specified from knowledge of the state of the ground and Table 4 which lists values of ground albedo for certain frequently occurring ground conditions. Table 4 was compiled from a number of different sources, but principally from Kondratyev (1969, 1973)<sup>62, 63</sup>, Robinson (1966)<sup>64</sup>, and the ASHRAE Handbook (1977)<sup>65</sup>.  $R_k$  and  $T_k$  are obtained from Eqs. (12) and (13). In applying these equations it is necessary to know  $\phi_k$ , a weighting function which depends upon the fractional cloud cover in layer  $k$  as well as cloud type and  $\cos z$ . Thus

$$\phi_k = W f_k \quad (15)$$

where  $W$  is a weighting function which depends upon cloud type, amount and  $\cos z$ .  $f_k$  is the fractional cloud cover of layer  $k$ . As indicated above,  $\phi_k = 0$  for  $f_k = 0$  and  $\phi_k = 1$  for  $f_k = 1.0$ . Thus if  $\phi_k$  is a linear function of  $f_k$  regardless of cloud type, then  $W = 1$  regardless of cloud type. Although this is usually the assumption made for  $W$  in applications such as general circulation models of the atmosphere, it is not, as we shall see, warranted by the observations, which show that  $\phi_k$  is not a linear function of  $f_k$  and that  $W$  may depart significantly from unity.

By choosing cloud-state situations in which only a single cloud type is present, it is possible to determine  $W$  from the SOLMET data for each cloud type, cloud fraction and  $\cos z$ . We examined three different situations.

<sup>62</sup> Kondratyev K. Ya., 1969: Radiation in the atmosphere. Int. Geophys. Series, Vol. 12., J. Van Mieghem, Ed. Acad. Press, N.Y., pp. 411-452.

<sup>63</sup> \_\_\_\_\_, (Ed.), 1973: Radiation characteristics of the atmosphere and the earth's surface. Russian Trans. NASA TT F-678, Amerind Pub. Co., New Delhi, pp. 192-223.

<sup>64</sup> Robinson, N., (Ed.), 1966: Solar radiation. Elsevier Pub. Co., Amsterdam. Chap. 6, pp. 196-221.

<sup>65</sup> ASHRAE, 1977: Handbook, Fundamentals. Am. Soc. Heat., Refrig. Air. Cond. Eng., N.Y., p. 2.9.

TABLE 4. ALBEDOS FOR VARIOUS SURFACES.

<u>SOILS</u>	<u>DRY</u>	<u>WET</u>	<u>WETNESS UNSPECIFIED OR INDIFFERENT</u>							
Dark	0.13	0.08								
Light	0.18	0.10								
Dark-ploughed	0.08	0.06								
Light-ploughed	0.16	0.08								
Clay	0.23	0.16								
Sandy	0.25	0.18								
Sand	0.40	0.20								
White sand	0.55									
<u>SURFACES</u>										
Asphalt			0.10							
Lava			0.10							
Tundra			0.20							
Steppe			0.20							
Concrete			0.30							
Stone			0.30							
Desert			0.30							
Rock	0.35	0.20								
Dirt road	0.25	0.18								
Clay road	0.30	0.20								
<u>FIELDS</u>		<u>GROWING</u>	<u>DORMANT</u>	<u>VERDURE UNSPECIFIED OR INDIFFERENT</u>						
Tall grass	0.18	0.13		0.16						
Mowed grass	0.26	0.19		0.22						
Desiduous trees	0.18	0.12		0.15						
Coniferous trees	0.14	0.12		0.13						
Rice	0.12									
Beet, wheat	0.18									
Potato	0.19									
Rye	0.20									
Cotton	0.21									
Lettuce	0.22									
<u>SNOW</u>		<u>ICE</u>								
Fresh	0.85		White	0.75						
Dense	0.75		Grey	0.60						
Moist	0.65		Snow and Ice	0.65						
Old	0.55		Dark glass	0.10						
Melting	0.35									
<u>WATER</u>										
COS Z										
	.95	.85	.75	.65	.55	.45	.35	.25	.15	.05
DIRECT RADIATION	.03	.03	.03	.04	.06	.08	.13	.23	.41	.76
TOTAL										
Calm	.03	.03	.03	.04	.06	.09	.12	.17	.24	.30
RADIATION Rough	.03	.03	.04	.05	.07	.08	.10	.12	.14	.15



(1) When the fractional cloud is in layer 1, from Eq. (9) we have

$$D_2 = 1 - R_2 R_3 - R_3 R_g + R_2 R_g (R_3^2 - T_3^2) - R_1 \left[ R_2 + R_3 (T_2^2 - R_2^2) - R_g \left\{ R_2 R_3 + R_3^2 (T_2^2 - R_2^2) + T_3^2 (R_2^2 - T_2^2) \right\} \right] \quad (16)$$

where we have arranged terms so as to factor the level 1 coefficient,  $R_1$ .

From Eq. (9) we also have

$$D_2 = T_1 T_2 T_3 X_0 / X_3 = T_1 T_2 T_3^* / X_3 \quad (17)$$

where  $X_3^*$  is merely the numerical fraction  $X_3 / X_0$ .

Choosing cases in which there are no clouds in layers 2 and 3, and in which there is neither precipitation nor obstruction to visibility, we obtain the values of  $R_2$ ,  $R_3$ ,  $T_2$ ,  $T_3$  which are required in Eqs. (16) and (17) from Table 2. We also know  $R_1$  and  $T_1$  for both clear and overcast states. Eqs. (12) and (13) express  $R_k$  and  $T_k$  for any cloud fraction as a function of the corresponding basic (clear and overcast) states, in terms of the unknown weighting function  $\phi_k$ . Eliminating  $D_2$  between Eqs. (16) and (17) and substituting for  $R_1$  and  $T_1$  from Eqs. (12) and (13) we have

$$\phi_1 = \frac{\left[ 1 - R_2 R_3 - R_3 R_g + R_2 R_g (R_3^2 - T_3^2) - \frac{T_2 T_3 t_1}{X_3^*} - r_1 \left\{ R_2 + R_3 (T_2^2 - R_2^2) - R_g \left[ R_2 R_3 + (R_3^2 - T_3^2) (T_2^2 - R_2^2) \right] \right\} \right]}{\left( \rho_1 - r_1 \right) \left\{ R_2 + R_3 (T_2^2 - R_2^2) - R_g \left[ R_2 R_3 + (R_3^2 - T_3^2) (T_2^2 - R_2^2) \right] \right\} + \frac{T_2 T_3 (t_1 - t_1)}{X_3^*}} \quad (18)$$

Using observed mean values of  $X_3^*$  from the 13 development stations we determined  $\phi_1$  for both thin and thick Ci/CS as a function of cloud fraction and  $\cos z$ . Using Eq. (15) we obtained the weights tabulated in Tables 5 and 6.

TABLE 5. VALUES OF THE WEIGHTING FUNCTION, W, FOR THIN Ci/Cs.

CLOUD FRACTION	COS Z							
	.15	.25	.35	.45	.55	.65	.75	.85
.1	.375	-.296	-.826	-1.405	-.804	.311	.443	-.272
.2	1.669	.516	.201	.114	.574	.935	.221	-.136
.3	1.334	.344	.338	.482	.209	.624	.521	.462
.4	1.133	.697	.223	.260	.384	.785	.471	.222
.5	1.169	.536	.568	-.009	.074	.459	.758	.145
.6	.755	.610	.654	.510	.321	.758	.659	.560
.7	.742	.646	.681	.609	.477	.809	.745	.715
.8	.764	.726	.850	.799	.658	.865	.869	.605
.9	.952	.741	.913	.842	.825	.954	.999	1.008

TABLE 6. VALUES OF THE WEIGHTING FUNCTION, W, FOR THICK Ci/Cs.

CLOUD FRACTION	COS Z							
	.15	.25	.35	.45	.55	.65	.75	.85
.1	1.594	1.143	.409	.638	.326	.778	.547	.255
.2	.777	.993	.678	.600	.401	.516	.357	.215
.3	.904	.788	.660	.500	.347	.497	.498	.027
.4	.834	.638	.669	.567	.355	.373	.429	.064
.5	.722	.727	.373	.547	.425	.470	.663	.468
.6	.911	.716	.831	.645	.733	.815	.770	.543
.7	.679	.744	.643	.718	.733	.663	.683	.676
.8	.604	.709	.642	.649	.827	.782	.665	.711
.9	.717	.626	.770	.749	.706	.851	.917	.836

(2) When the fractional cloud is in layer 2, the expression for  $\phi_2$  is a quadratic:

$$A_2 \phi_2^2 + B_2 \phi_2 + C_2 = 0 \quad (19)$$

where

$$A_2 = R_1 (R_3 - R_g R_3^2 + R_g T_3^2) (\rho_2^2 - \tau_2^2 + 2\tau_2 t_2 - 2\rho_2 r_2 + r_2^2 - t_2^2)$$

$$\begin{aligned}
B_2 &= (r_2 - \rho_2)(R_1 + R_3 - R_g R_3^2 + R_g T_3^2 - R_1 R_3 R_g) + \frac{T_1 T_3 (t_2 - \tau_2)}{X_3^*} \\
&\quad + 2R_1 (R_3 - R_g R_3^2 + R_g T_3^2) (\rho_2 t_2 - \tau_2 t_2 + t_2^2 - r_2^2) \\
C_2 &= 1 - R_3 R_g - r_2 (R_1 + R_3 - R_g R_3^2 + R_g T_3^2 - R_1 R_3 R_g) - \frac{T_1 T_3 t_2}{X_3^*} \\
&\quad + R_1 (R_3 - R_g R_3^2 + R_g T_3^2) (r_2^2 - t_2^2).
\end{aligned}$$

(3) When the fractional cloud is in layer 3, the expression for  $\phi_3$  is also a quadratic:

$$A_3 \phi_3^2 + B_3 \phi_3 + C_3 = 0 \quad (20)$$

where

$$\begin{aligned}
A_3 &= R_g (R_2 - R_1 R_2^2 + R_1 T_2^2) (\rho_3^2 - \tau_3^2 + 2\tau_3 t_3 - 2\rho_3 r_3 + r_3^2 - t_3^2) \\
B_3 &= (r_3 - \rho_3)(R_2 + R_g - R_1 R_2^2 + R_1 T_2^2 - R_1 R_2 R_g) + \frac{T_1 T_2 (t_3 - \tau_3)}{X_3^*} \\
&\quad + 2R_g (R_2 - R_1 R_2^2 + R_1 T_2^2) (\rho_3 r_3 - \tau_3 t_3 + t_3^2 - r_3^2) \\
C_3 &= 1 - R_1 R_2 - r_3 (R_2 + R_g - R_1 R_2^2 + R_1 T_2^2 - R_1 R_2 R_g) - \frac{T_1 T_2 t_3}{X_3^*} \\
&\quad + R_g (R_2 - R_1 R_2^2 + R_1 T_2^2) (r_3^2 - t_3^2).
\end{aligned}$$

In both Eqs. (19) and (20) the quadratic terms are so small that one of the solutions is always the same (to three decimal places) as the solutions obtained by neglecting the quadratic terms. Therefore there is no ambiguity in the proper choice of solution for  $\phi_k$ . Using Eq. (15) we obtained the weights tabulated in Tables 7, 8, and 9.

TABLE 7. VALUES OF THE WEIGHTING FUNCTION, W, FOR As/Ac.

CLOUD FRACTION	COS Z							
	.15	.25	.35	.45	.55	.65	.75	.85
.1	1.340	.931	.743	.794	.940	.681	.696	.471
.2	1.038	.777	.618	.447	.673	.603	.611	.452
.3	.813	.574	.642	.568	.488	.520	.423	.277
.4	.732	.624	.708	.487	.443	.402	.430	.286
.5	.827	.656	.670	.423	.541	.485	.433	.338
.6	.730	.763	.611	.626	.608	.550	.408	.488
.7	.643	.616	.631	.593	.652	.603	.581	.520
.8	.718	.782	.644	.630	.705	.630	.623	.623
.9	.839	.812	.734	.758	.718	.787	.751	.675

TABLE 8. VALUES OF THE WEIGHTING FUNCTION, W, FOR Sc/St.

CLOUD FRACTION	COS Z							
	.15	.25	.35	.45	.55	.65	.75	.85
.1	2.085	2.007	1.450	1.288	1.234	1.012	.716	.394
.2	1.208	1.140	.981	.925	.832	.712	.531	.426
.3	.827	.913	.789	.753	.744	.674	.533	.444
.4	.751	.791	.680	.803	.727	.665	.557	.507
.5	.697	.868	.756	.717	.669	.626	.579	.504
.6	.628	.800	.626	.636	.679	.649	.585	.522
.7	.817	.782	.653	.712	.633	.647	.640	.554
.8	.763	.857	.666	.737	.744	.723	.640	.653
.9	.861	.744	.773	.843	.818	.782	.771	.753

TABLE 9. VALUES OF THE WEIGHTING FUNCTION, W, FOR Cu/Cb.

CLOUD FRACTION	COS Z							
	.15	.25	.35	.45	.55	.65	.75	.85
.1	.533	.690	.342	.511	.386	.352	.389	.075
.2	.717	.564	.408	.367	.258	.359	.400	.115
.3	.750	.646	.413	.429	.272	.339	.310	.253
.4	.658	.565	.489	.458	.384	.371	.350	.250
.5	.521	.638	.368	.401	.465	.397	.369	.269
.6	.631	.579	.502	.518	.490	.503	.471	.441
.7	.648	.651	.593	.513	.498	.558	.555	.517
.8	.659	.655	.607	.592	.594	.589	.568	.570
.9	.742	.720	.692	.643	.655	.652	.676	.630

It is apparent from Eqs. (12) and (13) that a weight ( $W$ ) greater than 1.00 implies that the effect of the clouds (in terms of reflectivity or transmissivity coefficient) is stronger than would be indicated by the cloud fraction alone. Similarly, values of  $W$  less than 1.00 imply that the effect of the clouds is weaker than would be indicated by the cloud fraction alone. Values of  $W$  near 1.00 imply that the effect of clouds is nearly linear with cloud fraction. Negative values of  $W$  mean that more insolation reaches the ground with some clouds present than when the sky is completely clear. There are a few negative weights for small cloud fractions of cirrus or cirrostratus. On the other hand, for this same cloud type there are some weights greater than 1.00, especially when the sun is low in the sky. Negative weights do not occur with any of the other cloud types; however, cumulus clouds have the lowest average weight (0.496), which is probably due to the fact that there is frequent reflection of sunlight down to the ground from the sides of these clouds. Stratiform low clouds have the highest average weight (0.781), which is, nevertheless, considerably less than 1.00. Thus it is apparent that it is improper to assume that  $\phi_k$  is a linear function of cloud fraction.

## 5. APPLICATION OF THE MODEL

Routine synoptic observations contain all of the information needed to apply the solar insolation model; namely, type and amount of clouds, obstructions to visibility and precipitation. The proper choice of ground albedo may also be considered a function of present and past synoptic data insofar as they contain information on such considerations as snow on the ground or the wetness of the ground. The additional information needed for the choice of ground albedo from Table 4 is obtained from knowledge of the physiography and climatology of the location.

In addition to  $R_g$ , solution of Eq. (9) requires knowledge of  $R_k$  and  $T_k$  for the three layers ( $k = 1, 2, 3$ ). The model recognizes nine basic or uniform states, three in layer 1, two in layer 2, and four in layer 3. Each layer has a basic state in which the layer is clear. In addition, the bottom layer (layer 3) has a basic state consisting of smoke and/or fog occurring in conjunction with an otherwise clear layer 3. Added to these four clear-layer basic states, there are five overcast-layer

basic states: thin Ci/Cs or thick Ci/Cs in layer 1, As/Ac in layer 2 and either Cu/Cb or Sc/St in layer 3. All possible sky states including fractional cloudiness are represented by combinations of the basic states. Precipitation is assumed to be represented by overcast in all three layers: thick Ci/Cs in layer 1, As/Ac in layer 2, and Sc/St in layer 3.

The first step in the application of the model is to use the synoptic information to obtain  $R_g$  and the appropriate basic state values of  $R_k$  and  $T_k$ . If in any layer  $k$ , the cloud fraction is either 0 or 1, then only one basic state value is needed ( $r_k$  or  $\rho_k$ ) for  $R_k$  and ( $t_k$  or  $\tau_k$ ) for  $T_k$ . If, however, there are fractional clouds in layer  $k$  equal to or greater than 0.1 but less than or equal to 0.9, then both the clear and overcast basic state values are needed in order to determine the appropriate  $R_k$  and  $T_k$ .

The basic state values for  $R_k$  and  $T_k$  in Tables 2 and 3 are tabulated as mean values for each  $\cos z$  interval, which means that they are appropriate only for the midpoint values in each interval. Inasmuch as  $\cos z$  will be observed as a continuous variable, it is necessary to have a procedure for obtaining values for the basic state coefficients for intermediate values of  $\cos z$ . It was found that more than 98 percent of the variance of each basic state coefficient could be explained with a cubic polynomial in  $\cos z$ . Therefore, it was decided to use the cubic polynomial to obtain the basic state coefficients rather than storing the values of Tables 2 and 3 in the computer and interpolating for intermediate values of  $\cos z$ . The polynomial coefficients for each basic state for  $R_k$  and  $T_k$  are listed in Tables 10 and 11 respectively.

To obtain the basic state values of  $R_k$  and  $T_k$  from Tables 10 and 11 it is necessary to obtain  $\cos z$ .

$$\cos z = \sin \theta \sin D + \cos \theta \cos D \cos h \quad (21)$$

where  $\theta$  is the latitude,  $D$  is the declination, and  $h$  is the hour angle of the sun.  $h$  is the angle between the local meridian and the meridian of the sun. It is zero at local solar noon and -15 degrees or +15 degrees for every hour before or after local solar noon.

Step 1 in the application of the model is to determine the amounts and types of clouds in each of the three layers from the synoptic data and then to determine the values of  $r_k$  and  $t_k$  and/or  $\rho_k$  and  $\tau_k$  from the appropriate sets of polynomial coefficients. If any of the three layers

are not in a basic state condition it is necessary to use Eqs. (12) and (13) to obtain  $R_k$  and  $T_k$  for that layer. This means that we must determine  $\phi_k$  from Eq. (15). Again, it was found expedient to express  $W$  as a polynomial rather than apply two-dimensional interpolation to the values tabulated in Tables 5 through 9. It can be seen that these tables do not list values of  $W$  for  $\cos z = 0.05$  and  $0.95$ . In general there were too few cases for  $\cos z > .90$  to obtain reliable values for this category. Values of  $W$  for  $\cos z = 0.05$  are also unreliable because of the small values of  $X_0$  in the denominator of  $X_3^*$  which enter into the solution of  $\phi_k$ . By evaluating the polynomial coefficients from the more reliable values of  $W$  but applying the polynomials thus determined to all values of  $\cos z$ , we automatically avoid the problem of unreliability for extreme values of  $\cos z$ . Since  $W$  is a function of both cloud fraction as well as  $\cos z$ , we estimated the weights by means of a separate bi-quadratic polynomial for each cloud type. The coefficients are listed in Table 12. The fraction of the variance of  $W$  explained by the polynomials (0.69) is much smaller than that for  $R_k$  and  $T_k$ ; however, the calculation of  $\hat{X}_3$  is much less sensitive to  $W$  than to  $R_k$  and  $T_k$  and therefore it is felt that the accuracy in estimating  $W$  from the bi-quadratic polynomial is adequate. After determining appropriate values of  $W$ , appropriate values of  $R_k$  and  $T_k$  are found from Eqs. (12) and (13).

With diffuse radiation conditions, the appropriate basic state values of  $R_k$  and  $T_k$  are not functions of  $\cos z$  and therefore are not determined from the cubic polynomial. The diffuse basic state values are listed in Tables 2 and 3 under column D for layers 2 and 3. In using values of D in a layer containing fractional cloudiness, we assume that  $W = 1$ . Therefore,  $R_k$  and  $T_k$  for this layer are the proportionally weighted averages of the clear and overcast values of D.

After obtaining the seven parameters ( $R_1, R_2, R_3, R_9, T_1, T_2, T_3$ ) Eq. (9) is solved for  $\hat{X}_3$ , which is expressed in terms of  $X_0$ , the extra-terrestrial radiation per unit horizontal surface. To express  $\hat{X}_3$  in terms of energy received at the ground, we must evaluate  $X_0$ .

$$X_0 = S \left( \frac{\bar{d}}{d} \right)^2 \cos z \quad (22)$$

where  $S$  is the solar constant,  $d$  the distance and  $\bar{d}$  the mean distance of

the earth from the sun. According to Hoyt (1981)<sup>66</sup>, the best mean value for the quiet sun solar constant is 1369.2 W/m<sup>2</sup>.  $(\bar{d}/d)^2$  is a function of the ellipticity of the earth's orbit and the position of the earth in its orbit around the sun. It may be expressed as

$$(\bar{d}/d)^2 = \left[ 1.000140 + 0.016726 \cos \frac{2\pi(\text{JD}-2)}{365} \right]^2 \quad (23)$$

where JD, the Julian day, is 1 on January 1 and 365 on December 31.

TABLE 10. CUBIC POLYNOMIAL COEFFICIENTS FOR REFLECTIVITY ( $R_k$ ):  $r_k$  (clear layer) and  $\rho_k$  (overcast layer),  $k = 1, 2, 3$ .

	$R_k = a_0 + a_1 \cos z + a_2 \cos^2 z + a_3 \cos^3 z$			
	$a_0$	$a_1$	$a_2$	$a_3$
$r_1$	.12395	-.34765	.39478	-.14627
$r_2$	.15325	-.39620	.42095	-.14200
$r_3$	.15946	-.42185	.48800	-.18493
$r_3$ (F/K)	.27436	-.43132	.26920	-.00447
$\rho_1$ (THIN Ci/Cs)	.25674	-.18077	-.21961	.25272
$\rho_1$ (THICK Ci/Cs)	.60540	-.55142	-.23389	.43648
$\rho_2$ (As/Ac)	.66152	-.14863	-.08193	.13442
$\rho_3$ (Sc/St)	.71214	-.15033	.00696	.03904
$\rho_3$ (Cu/Cb)	.67072	-.13805	-.10895	.09460

NOTES:  $r_3$  (F/K) is used for the clear layer reflectivity of the bottom layer when fog and/or smoke are reported.

High clouds (layer 1) - any form of cirrus or cirrostratus or cirrocumulus - are distinguished only by thin or thick.

Middle clouds (layer 2) - all forms of middle clouds are governed by  $\rho_2$ .

Low clouds (layer 3) - we distinguish only between stratiform clouds (stratocumulus, stratus, nimbostratus) and convective clouds (cumulus, cumulonimbus).

<sup>66</sup> Hoyt, D. V., 1981: Personal communication.



TABLE 11. CUBIC POLYNOMIAL COEFFICIENTS FOR TRANSMISSIVITY ( $T_k$ ):  $t_k$  (clear layer) AND  $\tau_k$  (overcast layer),  $k = 1, 2, 3$ .

$$T_k = b_0 + b_1 \cos z + b_2 \cos^2 z + b_3 \cos^3 z$$

	$b_0$	$b_1$	$b_2$	$b_3$
$t_1$	.76977	.49407	-.44647	.11558
$t_2$	.69318	.68227	-.64289	.17910
$t_3$	.68679	.71012	-.71463	.22339
$t_3$ (F/K)	.55336	.61511	-.29816	-.06663
$\tau_1$ (THIN Ci/Cs)	.63547	.35229	.09709	-.22902
$\tau_1$ (THICK Ci/Cs)	.26458	.66829	.24228	-.49357
$\tau_2$ (As/Ac)	.19085	.32817	-.08613	-.08197
$\tau_3$ (Sc/St)	.13610	.29964	-.14041	.00952
$\tau_3$ (Cu/Cb)	.17960	.34855	-.14875	.01962

NOTES:  $t_3$  (F/K) is used for the clear-layer transmissivity of layer 3 when fog and/or smoke are reported.

Remaining comments same as those in Table 10.

TABLE 12. BI-QUADRATIC POLYNOMIAL COEFFICIENTS FOR THE WEIGHT (W) FOR EACH CLOUD TYPE AS A FUNCTION OF CLOUD FRACTION ( $f_k$ ) AND  $\cos z$ .

$$W = C_0 + C_1 \cos z + C_2 f_k + C_3 f_k \cos z + C_4 \cos^2 z + C_5 f_k^2$$

	$C_0$	$C_1$	$C_2$	$C_3$	$C_4$	$C_5$
THIN Ci/Cs	0.675	-3.432	1.929	0.842	2.693	-1.354
THICK Ci/Cs	1.552	-1.957	-1.762	2.067	0.448	0.932
As/Ac	1.429	-1.207	-2.008	0.853	0.324	1.582
Sc/St	0.858	-1.075	-0.536	0.750	0.322	0.501
Cu/Cb	2.165	-1.277	-3.785	2.089	-0.387	2.342

## 6. ANALYSIS OF ERROR AND CONCLUSIONS

Error analyses are derived separately for the 13 development stations and the 12 test stations as well as for all stations combined. Figure 3 shows the geographical distribution of the stations used for development of the reflectivity, absorptivity and transmissivity coefficients as well as the stations reserved for testing. Although the SOLMET tapes contained data for Omaha, NE and Stephenville, TX, these stations were not used. The cloud information for Omaha was missing and the data sample for Stephenville (which is close to Fort Worth) was too small to be useful.

Although the stations are designated as development and test stations only the so-called uniform cloud states were used in developing the coefficients. These states included clear skies (that is, less than 0.1 cloud cover) and overcast conditions where the first cloud layer visible from the ground was overcast. Of the total number of complete hourly observations available at the development stations (660504), less than 35 percent consisted of uniform cloud states as defined above. The remainder consisted of multi-layer cloud states and fractional cloud states. From the latter group, single-layer fractional cloud states were used to determine the weighting coefficients. These data represent less than 20 percent of the total development sample. Thus in testing the model within the development sample, more than 65 percent of the data is partially independent and nearly 50 percent of the data is wholly independent of the data used to develop the computational details. Nevertheless, we will refer to this sample as the developmental sample. The test sample, consisting of a comparable number of hourly observations (579839), is of course, completely independent.

Figures 5 and 6 show respectively, the root mean square error (RMSE) and the bias in the fraction of the extra-terrestrial solar radiation transmitted to the ground at each of the stations. RMSE is defined as

$$(\text{RMSE})_j = \left[ \frac{1}{N_j} \sum_{i=1}^{N_j} (\hat{X}_n - X_n)_{ij}^2 \right]^{1/2}$$

where  $N_j$  is the total number of hourly observations at station  $j$ ,  $\hat{X}_n$  is the computed value of the total insolation received at the ground and  $X_n$

A map of the Hawaiian Islands, including Johnston Atoll, Laysan Island, Midway Island, and the main Hawaiian Islands chain. The map is marked with numbered locations. A legend in the bottom right corner indicates that circles with a dot inside represent 'DEVELOPMENT STATIONS' and solid black dots represent 'TEST STATIONS'.

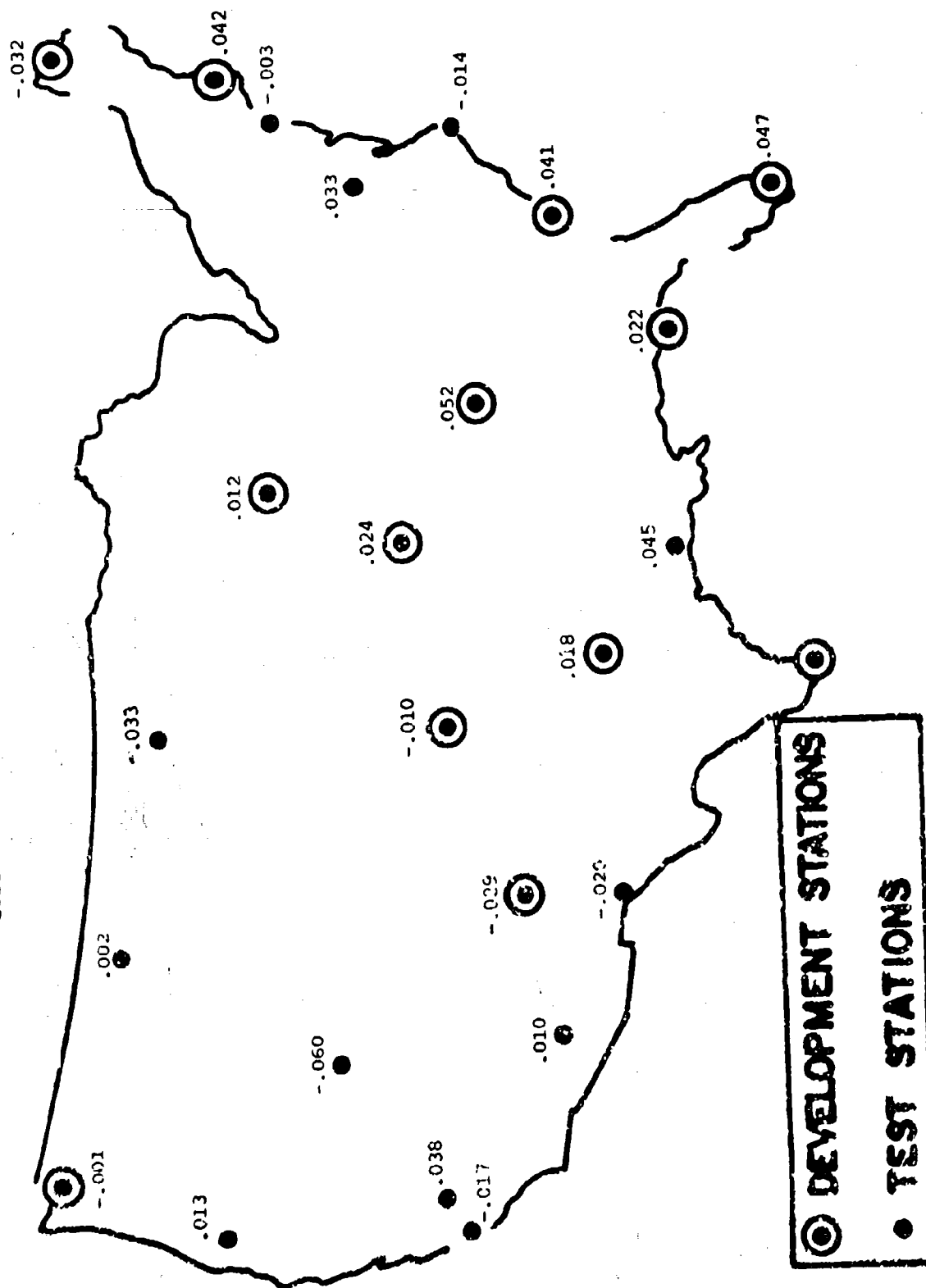
**Legend:**

- DEVELOPMENT STATIONS
- TEST STATIONS

**Numbered Locations:**

- Development Stations (Circles with dots):** 117, 122, 126, 129, 136, 141, 144, 146, 148, 161, 111, 120, 122, 129, 115, 118, 121, 125, 128, 130, 105, 096, 107, 108, 109, 110, 112, 113, 114, 116, 119, 123, 124, 127, 131, 132, 133, 134, 135, 137, 138, 139, 140, 142, 143, 145, 147, 149, 150, 151, 152, 153, 154, 155, 156, 157, 158, 159, 160, 162, 163, 164, 165, 166, 167, 168, 169, 170, 171, 172, 173, 174, 175, 176, 177, 178, 179, 180, 181, 182, 183, 184, 185, 186, 187, 188, 189, 190, 191, 192, 193, 194, 195, 196, 197, 198, 199, 200.
- Test Stations (Solid dots):** 101, 102, 103, 104, 106, 109, 110, 111, 112, 113, 114, 115, 116, 117, 118, 119, 120, 121, 122, 123, 124, 125, 126, 127, 128, 129, 130, 131, 132, 133, 134, 135, 136, 137, 138, 139, 140, 141, 142, 143, 144, 145, 146, 147, 148, 149, 150, 151, 152, 153, 154, 155, 156, 157, 158, 159, 160, 161, 162, 163, 164, 165, 166, 167, 168, 169, 170, 171, 172, 173, 174, 175, 176, 177, 178, 179, 180, 181, 182, 183, 184, 185, 186, 187, 188, 189, 190, 191, 192, 193, 194, 195, 196, 197, 198, 199, 200.

Figure 6. Bias of model calculations of fraction of extra-terrestrial solar radiation transmitted to ground.



is the observed value. Both  $X_n$  and  $\hat{X}_n$  are expressed as fractions of  $X_0$ , the solar radiation outside the atmosphere per unit horizontal surface.

The bias is simply

$$(\text{BIAS})_j = \frac{1}{N_j} \sum_{i=1}^{N_j} (\hat{X}_n - X_n)_{ij}$$

The combined values of RMSE for the development stations, test stations and all stations shown in Part A of Table 13 are obtained by combining the sums of the squares of all of the individual errors. That is,

$$\text{RMSE} = \left[ \frac{1}{N} \sum_{j=p}^q \sum_{i=1}^{N_j} (\hat{X}_n - X_n)_{ij}^2 \right]^{1/2}$$

where p, q, and N are respectively 1, 13, 660504 for the development stations; 14, 25, 579339 for the test stations; and 1, 25, 1240343 for all stations.

The slight improvement in both RMSE and BIAS (see Part A of Tables 13 and 14) for the test stations as compared with the development stations, although unexpected, undoubtedly represents a sampling fluctuation due to the different mix of stations in the two samples. However, it is gratifying to find the test results no worse than the partially dependent sample.

Although there is an overall positive bias of about 1 percent, it does not appear worthwhile to modify the coefficients inasmuch as the bias for the test stations is essentially zero. Furthermore, no geographical pattern of bias can be discerned from Figure 6.

RMSE and BIAS were evaluated as functions of fractional cloud cover, solar zenith angle, the number and distribution of cloud layers present and weather conditions. The results are shown in Tables 13 and 14. Not unexpectedly, the smallest error occurs with clear skies. The error increases with increasing cloud fraction up to nine-tenths cloud coverage and is somewhat smaller for overcast skies. Part of this distribution of RMSE is due to the fact that the clear and overcast categories are essentially without observer error in estimating sky cover. Judging from the distribution of error, this component of error appears to account for about 20 percent of the total RMSE. The remaining sources of error, which will be discussed later in this section, are obviously increasingly prominent with increasing sky cover.

TABLE 13. ROOT MEAN SQUARE ERROR OF MODEL CALCULATION OF FRACTIONAL TRANSMISSION OF SOLAR RADIATION TO THE GROUND FOR VARIOUS CONDITIONS.

A. FRACTIONAL CLOUD COVER												
	0.0	0.1	0.2	0.3	0.4	0.5	0.6	0.7	0.8	0.9	1.0	TOTAL
DEV	.088	.094	.101	.108	.119	.126	.136	.146	.155	.169	.144	.128
TEST	.079	.089	.099	.107	.115	.125	.132	.141	.149	.159	.148	.119
ALL	.083	.092	.100	.108	.117	.126	.134	.144	.153	.165	.146	.124
NUMBER OF CASES	354240	71261	60927	63950	54736	50939	51235	66998	85715	90771	289571	1240343

B. COS Z (INTERVALS CENTERED ON)												
	0.05	0.15	0.25	0.35	0.45	0.55	0.65	0.75	0.85	0.95		
DEV	.152	.129	.127	.124	.125	.122	.129	.126	.124	.131		
TEST	.144	.128	.124	.124	.120	.115	.113	.112	.108	.108		
ALL	.148	.128	.126	.124	.122	.119	.122	.120	.117	.122		
NUMBER OF CASES	68505	109368	121480	127508	160141	138167	163987	153979	133862	63346		

C. LAYERED CLOUD DISTRIBUTION							
	L	M	H	LM	LH	MH	LMH
DEV	.131	.135	.107	.155	.141	.135	.174
TEST	.139	.137	.104	.153	.134	.136	.161
ALL	.134	.136	.106	.154	.138	.136	.168
NUMBER OF CASES	261230	55017	144532	73503	164487	97713	89621

D. WEATHER		
	NO WEATHER	PRECIPITATION
DEV	.127	.141
TEST	.117	.159
ALL	.122	.148
NUMBER OF CASES	1108565	60012
		71766

TABLE 14. AVERAGE BIAS OF MODEL CALCULATION OF . . . . . MISSION OF  
SOLAR RADIATION TO GROUND FOR VARIOUS CONDITIONS.

A. FRACTIONAL CLOUD COVER

	0.0	0.1	0.2	0.3	0.4	0.5	0.6	0.7	0.8	0.9	1.0	TOTAL
DEV	-.003	.005	.004	.004	.011	.018	.022	.027	.039	.057	.028	.018
TEST	-.001	-.006	-.009	-.011	-.011	-.010	-.006	-.001	.008	.022	.005	.000
ALL	-.002	-.000	-.001	-.002	.003	.007	.010	.015	.026	.042	.018	.010

B. COS Z (INTERVALS CENTERED ON)

	0.05	0.15	0.25	0.35	0.45	0.55	0.65	0.75	0.85	0.95
DEV	.018	.027	.011	.004	.011	.014	.028	.027	.020	.029
TEST	.013	.012	-.006	-.014	-.007	-.006	-.008	-.007	.002	.004
ALL	.016	.020	.003	-.004	.002	.004	.019	.018	.011	.019

C. LAYERED CLOUD DISTRIBUTION

	L	M	H	LM	LH	MH	LMH	CLEAR
DEV	.011	.015	.000	.041	.036	.028	.070	-.003
TEST	-.016	-.004	-.017	.018	.012	.007	.043	-.001
ALL	.001	.006	-.008	.032	.027	.017	.058	-.002

D. WEATHER

	NO WEATHER	PRECIPITATION	FOG/SMOKE
DEV	.017	.011	.014
TEST	.001	-.021	-.012
ALL	.010	-.001	.001

To place these RMSE's in perspective we can compare them with the observed standard deviation ( $\sigma$ ) of  $X_n$  for comparable categories. The only strictly comparable category for which  $\sigma$  is available is that for clear skies. The  $\sigma$  for this category is 0.078, which is to be compared with the RMSE of 0.083. This means that for this category the error in the model calculation is about the same size as the variability of the observations. Inasmuch as the model yields a fixed value for a particular set of conditions, such as clear skies,  $\sigma$  represents a lower bound for RMSE. The small difference be-

tween 0.078 and 0.083 is largely accounted for by the small bias in the calculation for this category.

Another category that can be compared, although not with the same precision, is that for overcast skies. In this case RMSE is 0.146 whereas the average standard deviation of the observations for overcast skies is 0.129. However, the RMSE applies to all overcast sky states, including states with multiple cloud layers, whereas the  $\sigma$  pertains only to overcast sky states where the first cloud layer visible from the ground is overcast. If we examine Part C of Table 13 we find that RMSE is larger for conditions with multiple cloud layers. In view of this variation of RMSE with multiple cloud layers, the small difference between the RMSE of 0.146 and the  $\sigma$  of 0.129 would undoubtedly be diminished further if the RMSE category were available for the same "uniform" or single-layer overcast conditions for which the  $\sigma$  applies. In addition, we shall show that the "true" RMSE is even smaller than is indicated in Table 13.

From Part B of Table 13 it is apparent that except for the cases where the sun is close to the horizon, RMSE varies little with  $\cos z$ . This result indicates that the variability of  $X_n$  with  $\cos z$  is being properly handled by the model. The larger error for the lowest  $\cos z$  category is a consequence of the manner in which the SOLMET data were recorded and does not necessarily indicate poorer model performance.

As already indicated, RMSE is larger for multi-layered cloud states. This result is not unexpected inasmuch as with more complicated cloud states there is more opportunity for observer error. The last part of Table 13 shows the variation of RMSE with three weather states. While the error is larger when there is precipitation as compared with no weather or smoke or fog, the difference is not very large. Furthermore, the RMSE for precipitation is almost the same as that for overcast skies. Thus it appears that the presence of precipitation does not in itself appreciably increase the RMSE above that which is expected for overcast skies without precipitation.

Table 14 shows the bias as a function of the same parameters as in Table 13. The overall bias is about 1 percent positive indicating that the calculated radiation reaching the ground is slightly larger than the observed. The errors appear to be larger for the so-called developmental sample than for the test sample, but this difference is undoubtedly for-



tuitous. There appears to be an increase in bias with increasing fractional cloud cover. However, the bias for overcast skies is less than that for both 0.8 and 0.9 cloud cover. Since the calculated insolation for fractional cloud cover is a function of that for clear and overcast states, it seems likely that the apparent relationship between RMSE and cloud fraction is fortuitous. It is possible that improper values of the weighting factor  $W$  are contributing to the variation of RMSE with cloud cover, but if the  $W$  values were an important contributor it might be expected that the apparent relationship of RMSE and cloud cover would be enhanced in the test sample. It is obvious that such is not the case. In any event, the bias in the test sample if not in the overall sample is small enough to be ignored.

From Part B of Table 14 it is apparent that there is no consistent variation of bias with zenith angle. Therefore, here too we may assume that the effects of zenith angle are being handled appropriately.

From Part C, it appears that it might be possible to decrease the bias by modifying the coefficients for multi-cloud layers, particularly when clouds are present in all three layers. It is not obvious, however, that the benefits to be derived would be worth the added complexity in the computer code, especially since Part D indicates that the bias does not seem to depend heavily upon the state of present weather.

Judging from the results shown in Tables 13 and 14, along with the limited comparisons with comparable standard deviations, both the coefficients derived from the developmental sample and the procedure for calculating the solar radiation received at the ground produced successful results on completely independent data; that is, there was no loss in accuracy with independent data. This is not to say that both the coefficients and the methodology cannot be improved. However, questions on the desirability of such improvements in terms of their costs are beyond the scope of this report. Nevertheless, it is useful to examine the sources of error and to indicate possible avenues of improvement. Furthermore, as indicated above, we shall show that the "true" error (and for that matter the "true" standard deviation) is less than that indicated in Table 13.

The principal sources of error in RMSE can be classified as follows:

1. Observer error

2. Errors due to lack of information
3. Errors due to lack of representativeness
4. Measurement error
5. Errors due to model simplicity

We have already alluded to observer error. This arises largely from the human observer's inability to integrate accurately the fractional cloud cover of an individual cloud layer except for those cases where the layer is overcast or the sky is clear. In addition, observer error includes cases where the cloud type is inappropriately identified. There is little that can be done with the solar insolation model to reduce this source of error as long as all of the cloud and weather information is derived from standard ground-based observations.

Another important source of error due to the ground-based nature of the meteorological observations is the lack of cloud information for layers above the lowest overcast layer. A possible means of reducing this uncertainty and therefore minimizing this source of error would be to make use of available cloud analyses (such as the 3-D Nephanalysis of the Air Weather Service Global weather Central) which incorporate important additional sources of information such as satellite information. However, one of the principal virtues of this solar insolation model is that it depends only upon routine ground-based observations.

One source of error which is present in the results shown in Table 13, but which presumably would not be present in practice, concerns the ground albedo. Lacking specific information on the ground albedo within the SOLMET data sample, a fixed climatological mean value of 0.15 was used for all stations and all seasons. In practice, however, it can be expected that there would be more information available on ground albedo. The use of such information could only diminish RMSE, but of course would have no effect on  $\sigma$ . In those situations in which the actual ground albedo differed significantly from 0.15, the computed solar radiation at the ground could be appreciably modified by the use of the appropriate ground albedo. For example, with a low overcast and high sun elevation  $\hat{X}_3$  is about  $0.30 X_0$  with  $R_g = .15$  but  $\hat{X}_3$  increases to  $0.45 X_0$  with  $R_g = .65$ . For the same conditions but with low solar elevation angle,  $\hat{X}_3$  is less than  $0.12 X_0$  with  $R_g = .15$  but greater than  $0.19 X_0$  with  $R_g = .65$ .

Another source of error in the present results which would not be present in practice concerns the method of data tabulation in the SOLMET tapes. Some of the data, such as the pyrheliometric data, are integrated over an hour, but other data, such as the standard meteorological data, refer to a specific time period. In situations where the weather is changing rapidly, the weather observations for the assigned hour may not be representative of the insolation measurement for that hour.

A major source of error concerns the basic solar insolation data. Although gross errors were presumably eliminated from the SOLMET tapes, many inconsistencies and anomalies remain in the data.

All of the above sources of error contribute to the indicated RMSE in Table 13, but are not model errors; that is, they are not true errors as far as the model is concerned. How much of the indicated RMSE is due to such errors is impossible to say, but they must be appreciable. Many of these sources of error also contribute to the observed standard deviation so that it is clear that the "true" standard deviation is also smaller than is indicated by the data.

There are model errors, of course, and these are largely due to misrepresentations and simplifications of the radiation physics by the modeling assumptions. Prominent among these simplifications are (1) the truncation errors introduced by representing a continuous atmospheric medium with only three discrete layers, (2) the simple and arbitrary treatment of direct and diffuse radiation, (3) the assumption that the  $(R, T, A)$  coefficients are the same for upward as for downward directed radiation, (4) the neglect of moisture and aerosols as a function of time and place, (5) the implicit neglect of seasonal and geographical variations by using the same coefficients for all stations for all seasons, (6) the use of a limited number of basic cloud type categories, and (7) the treatment of solar radiation for all practical purposes as monochromatic.

All of the above simplifications and approximations can be reduced but only at the expense of increased model complexity.

In view of the errors in the observational data needed to evaluate improved  $(R, T, A)$  coefficients, such model improvements do not appear to be warranted at the present time. However, it is also appropriate to point out that in spite of the simplifications and approximations the model appears to estimate the solar radiation received at the ground with relatively little error.

# REFERENCES

1. Shapiro, R., 1972: Simple model for the calculation of the flux of solar radiation through the atmosphere. *Appl. Opt.*, 11, 760-764.
2. Paltridge, G. W. and C. M. R. Platt, 1981: Aircraft measurements of solar and infrared radiation and the microphysics of cirrus cloud. *Quart. J. Roy. Meteor. Soc.*, 107, 367-380.
3. Reynolds, D. W., T. H. Vonder Haar and S. K. Cox, 1975: The effect of solar radiation in the tropical troposphere. *J. Appl. Meteor.*, 14, 433-444.
4. Paltridge, G. W., 1973: Direct measurement of water vapor absorption of solar radiation in the free atmosphere. *J. Atmos. Sci.*, 30, 156-160.
5. \_\_\_\_\_, 1974: Infrared emissivity, shortwave albedo, and the microphysics of stratiform water clouds. *J. Geophys. Res.*, 79, 4053-4058.
6. Cox, S. K., T. H. Vonder Haar and V. Suomi, 1973: Measurements of absorbed shortwave energy in a tropical atmosphere, *Solar Energy*, 14, 169-173.
7. Drummond, A. J. and J. R. Hickey, 1971: Large-scale reflection and absorption of solar radiation by clouds as influencing earth radiation budgets, new aircraft measurements. *Proc. Int. Conf. Wea. Mod.*, Canberra, Sep 1971., *Am. Meteor. Soc.*, Boston, pp. 267-276.
8. Feigelson, E. M., 1966: Light and heat radiation in stratus clouds. *Israel Prog. Sci. Trans.*
9. Predoehl, M. C. and A. F. Spano, 1965: Airborne albedo measurements over the Ross Sea, October-November 1962. *Mon. Wea. Rev.*, 93, 687-696.
10. Hanson, K. J. and H. J. Viebrock, 1964: Albedo measurements over the Northeastern U.S. *Mon. Wea. Rev.*, 92, 223-234.
11. Roach, W. T., 1961: Some aircraft observations of fluxes of solar radiation in the atmosphere. *Quart. J. Roy. Meteor. Soc.*, 87, 346-363.
12. Robinson, G. D., 1958: Some observations from aircraft of surface albedo and the albedo and absorption of cloud. *Arch. Meteor. Geophys. Bioklimat.*, B9, 28-41.
13. Fritz, S. and T. H. MacDonald, 1951: Measurement of absorption of solar radiation by clouds. *Bull. Am. Meteor. Soc.*, 32, 205-209.
14. \_\_\_\_\_, 1950: Measurements of the albedo of clouds. *Bull. Am. Meteor. Soc.*, 31, 25-27.
15. Neiburger, M., 1949: Reflection, absorption and transmission of insolation by stratus clouds. *J. Meteor.*, 6, 98-104.
16. Reynolds, D. W., T. B. McKee and K. S. Danielson, 1978: Effects of cloud size and cloud particles on satellite-observed reflected brightness. *J. Atmos. Sci.*, 35, 160-164.

17. Platt, C. M. R., 1976: Infrared adsorption and liquid water content in stratocumulus clouds. *Quart. J. Roy. Meteor. Soc.*, 102, 515-522.
18. Welch, R. M., S. K. Cox and J. M. Davis, 1980: Solar radiation and clouds. *Meteor. Monogr.*, Vol. 17, No. 39, Am. Meteor. Soc., Boston, 96 pp.
19. Van De Hulst, H. C., 1980: Multiple light scattering, tables, formulas, and applications. Vol. 1, pp. 1-299. Vol. 2, pp 300-739. Acad. Press.
20. Fouquart, Y., W. M. Irvine and J. Lenoble, 1980: Standard procedures to compute atmospheric radiative transfer in a scattering atmosphere. Radiation Commission, IAMAP. Pub. by National Center for Atmospheric Research, Boulder, CO 80307.
21. Lenoble, J., 1977: Standard procedures to compute radiative transfer in a scattering atmosphere. Radiation Commission, IAMAP. Pub. by National Center for Atmospheric Research, Boulder, CO 80307.
22. Newinger, M. and K. Bähneke, 1981: Influence of cloud composition and cloud geometry on the absorption of solar radiation. *Contrib. to Atmos. Phys.*, 54, 370-382.
23. Platt, C. M. R., 1981: The effect of cirrus of varying optical depth on the extra-terrestrial net radiative flux. *Quart. J. Roy. Meteor. Soc.*, 107, 671-678.
24. Welch, R. M. and W. G. Zdunkowski, 1981a: The radiative characteristics of noninteracting cumulus cloud fields. Part I: Parameterization for finite clouds. *Contrib. to Atmos. Phys.*, 54, 258-272.
25. \_\_\_\_\_ and \_\_\_\_\_, 1981b: The radiative characteristics of noninteracting cumulus cloud fields. Part II: Calculations for cloud fields. *Contrib. to Atmos. Phys.*, 54, 273-285.
26. Fouquart, Y. and B. Bonnel, 1980: Computations of solar heating of the Earth's atmosphere: A new parameterization. *Contrib. to Atmos. Phys.*, 53, 35-62.
27. Leighton, H. G., 1980: Application of the delta-Eddington method to the absorption of solar radiation in the atmosphere. *Atmos.-Ocean.*, 18, 43-52.
28. Manton, M. J., 1980: Computations of the effect of cloud properties on solar radiation. *J. De Recherches Atmos.*, 14, 1-16.
29. Meador, W. E. and W. R. Weaver, 1980: Two-stream approximations to radiative transfer in planetary atmospheres: A unified description of existing methods and a new improvement. *J. Atmos. Sci.*, 37, 630-643.
30. Zdunkowski, W. G., R. M. Welch and G. Korb, 1980: An investigation of the structure of typical two-stream methods for the calculation of solar fluxes and heating rates in clouds. *Contrib. to Atmos. Phys.*, 53, 147-166.
31. Davis, J. M., S. K. Cox and T. B. McKee, 1979a: Total shortwave radiative characteristics of absorbing finite clouds. *J. Atmos. Sci.*, 36, 508-518.
32. \_\_\_\_\_, \_\_\_\_\_ and \_\_\_\_\_, 1979b: Vertical and horizontal distribu-

- tions of solar absorption in finite clouds. *J. Atmos. Sci.*, 36, 1976-1984.
33. Liou, K.-N. and G. D. Wittman, 1979: Parameterization of the radiative properties of clouds. *J. Atmos. Sci.*, 36, 1261-1273.
  34. Schaller, A., 1979: A delta two-stream approximation in radiative flux calculations. *Contrib. to Atmos. Phys.*, 52, 17-26.
  35. Schmetz, J. and E. Raschke, 1979: An application of a two-stream approximation to calculations of the transfer of solar radiation in an atmosphere with fractional cloud cover. *Contrib. to Atmos. Phys.*, 52, 151-160.
  36. Stephens, G. L., 1978: Radiation profiles in extended water clouds. I: Theory. *J. Atmos. Sci.*, 35, 2111-2122.
  37. \_\_\_\_\_, 1979: Optical properties of eight water cloud types. CSIRO, *Atmos. Phys. Tech. Pap. No. 36*, 35pp.
  38. Davies, R., 1978: The effect of finite geometry on the three-dimensional transfer of solar irradiance in clouds. *J. Atmos. Sci.*, 35, 1712-1725.
  39. Kerschgens, M., U. Pilz and E. Raschke, 1978: A modified two-stream approximation for computations of the solar radiation budget in a cloudy atmosphere. *Tellus*, 30, 429-435.
  40. Twomey, S., 1976: Computations of the absorption of solar radiation by clouds. *J. Atmos. Sci.*, 33, 1087-1091.
  41. \_\_\_\_\_, 1977: Influence of pollution on the shortwave albedo of clouds. *J. Atmos. Sci.*, 34, 1149-1152.
  42. Wendling, P., 1977: Albedo and reflected radiance of horizontally inhomogeneous clouds. *J. Atmos. Sci.*, 34, 642-650.
  43. Wiscombe, W. J., 1976a: Extension of the doubling method to inhomogeneous sources. *J. Quant. Spectros. Radiat. Transfer*, 16, 477-489.
  44. \_\_\_\_\_, 1976b: On initialization error and flux conservation in the doubling method. *J. Quant. Spectros. Radiat. Transfer*, 16, 637-658.
  45. \_\_\_\_\_, 1977: The delta-M method: Rapid yet accurate radiative flux calculations for strongly asymmetric phase functions. *J. Atmos. Sci.*, 34, 1408-1422.
  46. Liou, K. -N., 1974: On the radiative properties of cirrus in the window region and their influence on remote sensing of the atmosphere. *J. Atmos. Sci.*, 31, 522-532.
  47. \_\_\_\_\_, 1976: On the absorption, reflection and transmission of solar radiation in cloudy atmospheres. *J. Atmos. Sci.*, 33, 798-805.
  48. McKee, T. B. and S. K. Cox, 1974: Scattering of visible radiation by finite clouds. *J. Atmos. Sci.*, 31, 1885-1892.
  49. \_\_\_\_\_ and \_\_\_\_\_, 1976: Simulated radiance patterns for finite cubic clouds. *J. Atmos. Sci.*, 33, 2014-2020.
  50. Welch, R. M., J. F. Geleyn, W. G. Zdunkowski and G. Korb, 1976: Radiative transfer of solar radiation in model clouds. *Beitr. Phys. Atmosph.*, 49, 128-146.

51. Wiscombe, J. J. and G. W. Grams, 1976: The backscattered fraction in two-stream approximations. *J. Atmos. Sci.*, 33, 2440-2451.
52. Zdunkowski, W. G. and G. Korb, 1974: An approximate method for the determination of short-wave radiative fluxes in scattering and absorbing media. *Beitr. Phys. Atmosph.*, 47, 129-144.
53. Haurwitz, B., 1948: Insolation in relation to cloud type. *J. Meteor.*, 5, 110-113.
54. Kasten, F. and G. Czeplak, 1980: Solar and terrestrial radiation dependent on the amount and type of cloud. *Solar Energy*, 24, 177-190.
55. Atwater, M. A. and J. T. Ball, 1978: A numerical solar radiation model based on standard meteorological observations. *Solar Energy*, 21, 163-170.
56. Tabata, S., 1964: Insolation in relation to cloud amount and sun's altitude. *Studies in Oceanography, Hidaka Volume*, 202-210.
57. Lumb, F. E., 1964: The influence of cloud on hourly amounts of total solar radiation at the sea surface. *Quart. J. Roy. Meteor. Soc.*, 90, 43-56.
58. Vowinckel, E. and S. Orvig, 1962: Relations between solar radiation and clouds. *Meteor. Monogr.*, Vol. 17, No. 39, Am. Meteor. Soc., Boston, 96pp.
59. SOLMET, 1977: Hourly solar radiation - surface meteorological observations. Vol. 1 - Users Manual. Vol. 2, 1979, Final Report. National Climatic Center, NOAA, EDIS, TD-9724.
60. Atwater, M. A. and J. T. Ball, 1981: A surface solar radiation model for cloudy atmospheres. *Mon. Wea. Rev.*, 109, 878-888.
61. Hoyt, D. V., 1979: An error in the rehabilitation of the National Weather Service solar radiation data. *Solar Energy*, 23, 557-559.
62. Kondratyev, K. Ya., 1969: Radiation in the atmosphere. *Int. Geophys. Series*, Vol. 12., J. Van Mieghem, Ed., Acad. Press, N.Y., pp 557-559.
63. \_\_\_\_\_, (Ed.), 1973: Radiation characteristics of the atmosphere and the Earth's surface. *Russian Trans. NASA TT F-678, Amerind Pub. Co.*, New Delhi, pp. 192-223.
64. Robinson, N., (Ed.), 1966: Solar radiation. *Elsevier Pub. Co.*, Amsterdam. Chap. 6, pp. 196-221.
65. ASHRAE, 1977: Handbook, Fundamentals. *Am. Soc. Heat., Refrig. Air. Cond. Eng.*, N.Y., p. 2.9.
66. Hoyt, D. V., 1981: Personal communication.